Neurobiology of Disease 127 (2019) 13–31

Contents lists available at ScienceDirect

Neurobiology of Disease

journal homepage: www.elsevier.com/locate/ynbdi

The presence and suppressive activity of myeloid-derived suppressor cells are potentiated after interferon-β treatment in a murine model of multiple sclerosis

Carolina Melero-Jerez[a,b,1], Margarita Suardíaz[c,2], Rafael Lebrón-Galán[a,2], Carmen Marín-Bañasco[c], Begoña Oliver-Martos[c], Isabel Machín-Díaz[a], Óscar Fernández[c], Fernando de Castro[b,*,1,2], Diego Clemente[a,**,1,2]

[a] Grupo de Neuroinmuno-Reparación, Hospital Nacional de Parapléjicos, Finca La Peraleda s/n, 45071 Toledo, Spain
[b] Grupo de Neurobiología del Desarrollo-GNDe, Instituto Cajal-CSIC, Avenida Doctor Arce 37, 28002 Madrid, Spain
[c] Unidad de Gestión Clínica Inter-centros de Neurociencias, Laboratorio de Investigación y Servicio de Neurología, Instituto de Investigación Biomédica de Málaga (IBIMA), Hospital Regional Universitario de Málaga, Madrid, Spain

ARTICLE INFO

Keywords:
IFN-β
EAE
Immunosuppression
Remyelination
Arginase-I
Inflammation
Immunomodulation

ABSTRACT

Multiple sclerosis (MS) is an autoimmune demyelinating disease of the human central nervous system (CNS), mainly affecting young adults. Among the immunomodulatory disease modifying treatments approved up to date to treat MS, IFN-β remains to be one of the most widely prescribed for the Relapsing-Remitting (RR) variant of the disease, although its mechanism of action is still partially understood. RR-MS variant is characterized by phases with increasing neurological symptoms (relapses) followed by periods of total or partial recovery (remissions), which implies the existence of immunomodulatory agents to promote the relapsing-to-remitting transition. Among these agents, it has been described the immunosuppressive role of a heterogeneous population of immature myeloid cells, namely the myeloid-derived suppressor cells (MDSCs) during the clinical course of the experimental autoimmune encephalomyelitis (EAE), the most used MS model to study RRMS. However, it is still unknown how the current MS disease modifying treatments, *e.g.* IFN- β, affects to MDSCs number or activity. Our present results show that a single injection of IFN-β at the onset of the clinical course reduces the severity of the EAE, enhancing the presence of MDSCs within the smaller demyelinated areas. Moreover, the single dose of IFN-β promotes MDSC immunosuppressive activity both *in vivo* and *in vitro*, augmenting T cell apoptosis. Finally, we show that IFN-ß preserves MDSC immaturity, preventing their differentiation to mature and less suppressive myeloid cell subsets. Taking together, all these data add new insights into the mechanism of IFN-β treatment in EAE and point to MDSCs as a putative endogenous mediator of its beneficial role in this animal model of MS.

1. Introduction

The most frequent primary demyelinating disease is multiple sclerosis (MS), an autoimmune, inflammatory and chronic disease of the central nervous system (CNS) that affects about 2,500,000 people worldwide (Sospedra and Martin, 2005). The clinical onset of MS typically occurs between 20 and 40 years of age and it is characterized by demyelination, axonal damage, oligodendrocyte death and neurological affectations. Relapsing-remitting MS (RRMS) is the most frequent form of the disease, in which an exacerbation of the symptoms (relapses) is followed by phases of remission. This would suggest the existence of molecules or specific cell types that control the immune system's activity (Meyer et al., 2017; Weissert, 2017), and eventually, (re)myelination. Murine experimental autoimmune encephalomyelitis (EAE) is the most common animal model for MS and it is based on a MHC class II-restricted $CD4^+/CD8^+$ T-cell mediated self-reaction against components of myelin (Glenn et al., 2014; Mastorodemos et al., 2015). Once in the CNS, T cells and microglia stimulated by this reaction recruit other immune cells from the circulating blood into the CNS, such as neutrophils and macrophages (Alabanza et al., 2013; Brown, 2007). The

* Correspondence to: F. de Castro, Grupo de Neurobiología del Desarrollo-GNDe, Instituto Cajal-CSIC, Avenida Doctor Arce 37, E-28002 Madrid, Spain.
** Correspondence to: D. Clemente, Grupo de Neuroinmuno-Reparación, Hospital Nacional de Parapléjicos, Finca *"La Peraleda"* s/n, E-45071 Toledo, Spain.
E-mail addresses: fdecastro@cajal.csic.es (F. de Castro), dclemente@sescam.jccm.es (D. Clemente).
[1] Former address: Grupo de Neurobiología del Desarrollo-GNDe, Hospital Nacional de Parapléjicos, Finca La Peraleda s/n, 45071 Toledo, Spain.
[2] These authors contributed equally to this work.

https://doi.org/10.1016/j.nbd.2019.02.014
Received 9 May 2018; Received in revised form 13 December 2018; Accepted 20 February 2019
Available online 21 February 2019

inflammatory reaction within the CNS leads to focal demyelination and oligodendrocyte death, followed by axonal damage. Interestingly, the existence of remitting phases in the EAE models implies the existence of immune-modulation that has been associated with the activity of different cell types: regulatory T cells (Treg; both $CD4^+$ and $CD8^+$), M2 macrophages, γδT cells and activated invariant NKT cells (Koutrolos et al., 2014; Ortega et al., 2013; Parekh et al., 2013). However, the role of a novel population of regulatory myeloid cells, namely myeloid-derived suppressor cells (MDSCs), and their activity in the context of EAE is still only partially understood (Melero-Jerez et al., 2016; Moliné-Velázquez et al., 2011; Moliné-Velázquez et al., 2014; Moline-Velazquez et al., 2016).

A standardized nomenclature has been established to describe the two main populations of MDSCs based on their morphological and phenotypical features (Bronte et al., 2016): i) polymorphonuclear or granulocytic MDSCs (PMN-MDSCs or G-MDSCs), defined as $CD11b^+Ly\text{-}6C^{low}Ly\text{-}6G^{high}$; and ii) monocytic MDSCs (M-MDSCs), of a $CD11b^+Ly\text{-}6C^{high}Ly\text{-}6G^{-/low}$ phenotype. Due to the difficulty in the discrimination of PMN-MDSCs from mature neutrophils (Bronte et al., 2016), the research on MDSCs in EAE has been mainly centralized on M-MDSCs (Moliné-Velázquez et al., 2011; Moliné-Velázquez et al., 2014; Zhu et al., 2007; Zhu et al., 2011), which indeed show a higher immunosuppressive activity when assessed in a per cell analysis (Dolcetti et al., 2010; Movahedi et al., 2008; Youn et al., 2008). In EAE, M-MDSCs have been described to be $CD11b^+Ly\text{-}6C^{high}Ly\text{-}6G^{-/low}$ in both the spleen and CNS of the mice at the peak of their clinical course (Moliné-Velázquez et al., 2011; Zhu et al., 2007, 2011). MDSCs share their phenotype with inflammatory immature monocytes, which are highly plastic during the immune processes that drive EAE. In fact, half of the $CD11b^+Ly\text{-}6C^{high}Ly\text{-}6G^{-/low}$ cells associated with the onset of the clinical course behave as MDSCs by suppressing the inflammatory process at the peak of the disease (Giles et al., 2018; Zhu et al., 2011). MDSCs exert their effects on T cells by either inhibiting their proliferation or by inducing their anergy/apoptosis through cell-cell interactions, and with maximal activity at the peak of clinical disability (Moliné-Velázquez et al., 2011). T cell proliferation is suppressed by the production of Arginase-I (Arg-I: Moliné-Velázquez et al., 2011) and nitric oxide (NO) by MDSCs in an Interferon-γ (IFN-γ) mediated manner (Zhu et al., 2007, 2011), and can be antigen-specific (Casacuberta-Serra et al., 2016). In healthy conditions, MDSCs present in the bone marrow normally polarize towards the different mature myeloid cell subsets. However, in cancer, but also in the context of EAE, MDSC differentiation is arrested, which is crucial to exert their potent immunosuppressive role in this animal model of MS (Gabrilovich et al., 2012; Moliné-Velázquez et al., 2011). The use of induced MDSCs in future therapeutic strategies is an active field of research in MS (Casacuberta-Serra et al., 2017; Gomez et al., 2014). However, in the case of endogenous MDSCs from MS patients (Iacobaeus et al., 2018) it will be important to check the unexplored effects of established molecular therapies for MS on this very plastic immune cell type.

Type I IFN-β is still used as the first line treatment for MS (Prinz et al., 2008) and it successfully reduces the frequency of clinical exacerbations by about 35% in patients at the onset of their neurological symptoms who are likely to convert into clinically defined-MS. Indeed, IFN-β decreases the lesion load as measured by MRI and it delays the progression of neurological disability (Arnason, 2005; Comi et al., 2001). The role of IFN-ß as a disease ameliorating agent in EAE has been explored extensively (Galligan et al., 2010; Martin-Saavedra et al., 2007; Suardíaz et al., 2016). As such, IFN-ß reduces the proliferation of autoreactive $CD4^+$ T cells against myelin epitopes (Gallina et al., 2006), it affects inflammatory cell infiltration by preserving the blood-brain barrier (BBB: Cheng et al., 2015; Stone et al., 1995), it interferes with the production of matrix metalloproteinases (Mastronardi et al., 2004; Waubant et al., 2003), it reduces the $CD4^+$ T-cell production of proinflammatory cytokines like IFN-γ (Mastronardi et al., 2004; Waubant et al., 2003), it inhibits Th17 polarization, it induces Th2 cell immune shifting (Kozovska et al., 1999), and it modifies the cytokine and chemokine expression profile during EAE (Cheng et al., 2015; Galligan et al., 2010; Martin-Saavedra et al., 2007; Sweeney et al., 2011; for a review see Kasper and Reder, 2014).

Myeloid cells represent potential targets for endogenously produced IFN-ß. The multiple effects of type I interferons on different myeloid subsets are well established (Brendecke and Prinz, 2012), both during the hematopoietic processes (Sonda et al., 2011) and in pathological conditions. Indeed, selective defects in one of its receptor subunits (IFNAR1) on myeloid cells leads to a severe disease, with a deteriorated effector phase and enhanced lethality (Prinz et al., 2008). Importantly, monocytes and macrophages, and their equivalent within the CNS, microglia, are IFNAR-dependent cells with pivotal roles in CNS immunity. Furthermore, IFNAR signaling participates in the myelin phagocytosis at the cellular level (Prinz et al., 2008). However, there is no data about the effect of IFN-β in MDSCs.

In the current study, we present novel data in the context of EAE indicating that the immunosuppressive activity of MDSCs is promoted after IFN-ß treatment, adding new insights into the modulation of MDSCs and providing a new perspective that could have important therapeutic consequences for the development of future cell-based therapies for MS.

2. Materials and methods

2.1. Induction of EAE

For *in vivo* IFN-ß treatment, female six-week-old C57/BL6 mice were purchased from Harlan Laboratories (Harlan, Udine, Italy). Chronic Progressive EAE was induced by subcutaneous immunization with 200 μg of Myelin Oligodendrocyte Glycoprotein ($MOG_{35–55}$ peptide: GenScript. New Jersey, USA) emulsified in complete Freund's adjuvant (CFA) containing 4 mg of heat inactivated *Mycobacterium tuberculosis* (BD Biosciences, Franklin Lakes, New Jersey, USA) and at a final volume of 200 μl. Immunized mice were administered Pertussis toxin (250 ng/mouse, Sigma-Aldrich, St. Louis, MO, USA), injected intravenously through the tail vein on the day of immunization and 48 h later. EAE was scored clinically on a daily basis in a double-blind manner as follows: 0, no detectable signs of EAE; 1, paralyzed tail; 2, weakness or unilateral partial hindlimb paralysis; 3 complete bilateral hindlimb paralysis; 4, total paralysis of forelimbs and hindlimbs; and 5, death.

At the onset of the symptoms (described as a clinical score between 0.5 and 1.5), EAE-induced animals received a single intraperitoneal injection of 10,000 units (40 ng) recombinant murine IFN-ß (Mouse Interferon Beta, mammalian, carrier-free: PBL Interferon source, Piscataway, NJ, USA) resuspended in 200 μl of saline, and they were sacrificed three days later with a lethal dose of pentobarbital.

All animal manipulations were approved by the institutional ethical committees (*Comité de Ética de la Investigación Provincial de Málaga* and *Comité Ético de Experimentación de la Universidad de Málaga,* and *Comité Ético de Experimentación Animal del Hospital Nacional de Parapléjicos*), and all experiments were performed in compliance with the European guidelines for animal research (European Communities Council Directives 2010/63/EU, 90/219/EEC, Regulation (EC) No. 1946/2003), and with the Spanish National and Regional Guidelines for Animal Experimentation and the Use of Genetically Modified Organisms (RD 53/2013 and 178/2004, Ley 32/2007 and 9/2003, Decreto 320/2010).

2.2. Immunohistochemisty

After sacrifice, fresh segments of the thoracic spinal cord were placed in 4% paraformaldehyde (PFA: Sigma-Aldrich) for 48 h at room temperature (RT). After immersion in 30% (w/v) sucrose diluted in 0.1 M Phosphate Buffer, pH 7.4 (PB) for 12 h, coronal cryostat sections

Table 1
List of antibodies and reagents used in this study.

Use	Antibody/Reagent	Target	Tissue/cells	Dilution	Class	Clone	Manufacturer	Antibody ID
Flow cytometry	CD11b-PerCP Cy5.5	Myeloid cells	Splenocytes	0.4 μg[a]	Rat monoclonal	M1/70	BD Biosciences	**AB-2394002**
	Ly-6C-FITC^{high} Ly-6G-PE$^{-/low}$	MDSCs	Splenocytes	Ly-6C: 1 μg[a] Ly-6G: 0.4 μg[a]	Rat monoclonal	Ly-6C: AL-21 Ly-6G: 1A8	BD Biosciences	**AB-394628** **AB-394206**
	F4/80-eFluor450	Macrophages	Splenocytes	0.4 μg[a]	Rat monoclonal	BM8	eBioscience	**AB-1548747**
	CD11c-APC	Dendritic cells	Splenocytes	0.4 μg[a]	Hamster monoclonal	N418	eBioscience	**AB-469346**
	CD3-PB	T cells	Splenocytes	0.4 μg[a]	Hamster monoclonal	500A2	BD Biosciences	**AB-397063**
	CD69-APC	Early activated T cells	Splenocytes	0.4 μg[a]	Hamster monoclonal	H1.2F3	eBioscience	**AB-1210795**
	Propidium iodide (PI/ RNase solution)	Dead/SubG1 cells	Splenocytes	–	–	–	Immunostep	
Histology	CD11b	Myeloid cells	SC	1:10	Rat monoclonal	M1/70.15	AbD, Serotec	**AB-321293**
	Arginase-I (V-20)	MDSCs and M2 cells	SC	1:100	Goat polyclonal		SCBT	**AB-2227469**
	Gr-1	MDSCs, Granulocytes	SC	1:10 (TSA 1:100)	Rat polyclonal	RB6-8C5	BD Biosciences	**AB-393586**
	CD124	MDSCs and M2 cells	SC	1:100	Mouse monoclonal	25,463	R&D Systems	**AB-2126871**
	TUNEL	Apoptotic cells	SC	Tdt enzyme 50%	-	-	Millipore	**AB-467067**
	CD4	CD4$^+$ T-cells	SC	1:25	Rat monoclonal	RM4–5	eBioscience	
	MHC-II	Antigen presenting cells	SC		Mouse monoclonal	M5/114.15.2	eBioscience	**AB-467560**
	PD-L1	Programmed death-ligand 1	SC	1: 100 (4 days of incubation)	Mouse monoclonal	MIH5	eBioscience	**AB-467780**

Abbreviations: APC, allophycocyanin; FITC, fluorescein isothiocyanate; PE, phycoerythrin; PB, pacific blue; SC, spinal cord; SCBT, Santa Cruz Biotechnology; TdT, terminal deoxynucleotidyl transferase; TSA, tyramide signal amplification.
[a] Refers to amount per million cells.

(20 μm thick: Leica, Nussloch, Germany) were thaw-mounted on Superfrost®Plus slides. After several rinses with PB, the sections were pre-treated for 15 min with 10% methanol in PB and they were pre-incubated for 1 h at RT in incubation buffer: 5% appropriate normal serum (Vector, Burlingame, USA) and 0.2% Triton X-100 (Merck) diluted in phosphate buffered saline (PBS). Immunohistochemistry was performed by incubating the sections overnight at 4 °C with the primary antibodies diluted in incubation buffer (Table 1). After rinsing, the sections were then incubated with the corresponding fluorescent (1:1000, Invitrogen, Paisley, UK) or biotinylated (1:200, Vector) secondary antibodies in incubation buffer for 1 h at RT. For Gr-1 staining, antibody binding was detected with biotinylated secondary antibody followed by the Vectastain Elite ABC reagent (Vector) and a FITC-labeled Streptavidin (Jackson ImmunoResearch, Suffolk, UK). In the case of Gr-1, additional blockade of endogenous avidin and biotin was performed prior to primary antibody incubation. For PD-L1 staining, primary antibodies were incubated during 96 h. Apoptosis was assayed by TUNEL, using the ApoTag® Plus Fluorescein *in situ* Apoptosis Detection Kit (Millipore, Billerica, MA, USA) according to manufacturer's instructions. In all cases, cell nuclei were stained with Hoeschst 33,342 (10 μg/ml, Sigma-Aldrich) and the sections were mounted with coverslips in Fluoromount-G (Southern Biotech, Birmingham, AL, USA).

2.3. Cell count and fluorescence intensity measurement

The total number of cells within the CNS tissue was assessed using a Leica confocal microscopy application (Suite 2.7.0 R1), manually couting cells in 3 sections (separated by 340 μm) of spinal cord from each animal. Pictures were acquired with a confocal SP5 microscope located at the Microscopy Service of the *Hospital Nacional de Parapléjicos,* with a *z* distance between planes of 1 μm, and cells were counted avoiding their overlap. All the lesions in the section were included in the analysis, and the total number of cells was considered in terms of the infiltrated area (measured with ImageJ software). Cellular positive labeling was considered only when it clearly surrounds a cell nucleus. For Gr-1, CD124, MHC-II and PD-L1 staining, we analyzed the intensity of fluorescence, measuring the average pixel intensity of 15–20 cells per lesion with ImageJ measurement tool.

2.4. Flow cytometry analysis of splenic populations

Fresh spleens from MOG-immunized mice were obtained at the peak of their clinical symptoms or three days after IFN-ß administration. The tissue was homogenized to single cell suspension, passed through a 40 μm nylon cell strainer (BD Biosciences) and washed in RPMI medium (Gibco-Thermo Fisher Scientific, Waltham, MA USA) supplemented with 10% heat-inactivated Fetal Bovine Serum (FBS: Gibco) and 1% penicillin/streptomycin (P/S: Gibco). After erythrocyte lysis in ACK lysis buffer (8.29 g/l NH_4Cl, 1 g/l $KHCO_3$, 1 mM EDTA in distilled H_2O at pH 7.4: Panreac, Barcelona, Spain), 2×10^6 splenocytes were re-suspended in 50 μl of staining buffer (sterile 1× PBS supplemented with 10% FBS, 25 mM HEPES buffer and 2% P/S: Gibco) and the Fc receptors were blocked for 10 min at 4 °C with anti-CD16/CD32 antibodies (10 μg/ml: BD Biosciences). After blocking, the cells were labeled for 30 min at 4 °C in the dark with 50 μl of the corresponding antibody panel in staining buffer (Table 1): a Pacific Blue conjugated hamster anti-mouse CD3, a FITC conjugated rat anti-mouse Ly-6C, a R-PE conjugated rat anti-mouse Ly-6G, a PErCP-Cy5.5 conjugated rat anti-mouse CD11b (all from BD Biosciences), an APC conjugated hamster anti-mouse CD69, an APC conjugated mouse anti-mouse CD11c, and an e-Fluor-450 conjugated mouse anti-mouse F4/80 (from eBioscience-Thermo Fisher Scientific). The splenocytes were then washed twice with staining buffer, recovered by centrifugation at 1500 rpm for 5 min at RT, resuspended in PBS and finally passed through a FACS Canto II cytometer (BD Biosciences) located at the Flow Cytometry Service of the *Hospital Nacional de Parapléjicos*. Both the percentages and the mean fluorescence intensity (MFI) of the cells were analyzed using FlowJo 7.6.4 software (Tree Star Inc. Ashaland, OR, USA).

2.5. Isolation of splenic Ly-6C^{high}-cells/MDSCs and T lymphocytes

Splenocytes were obtained from control (for T lymphocytes) or MOG-immunized C57BL/6 mice either at the onset (clinical score 0.5–1.5) or at the peak of clinical score (≥3 for MDSCs), as described previously (Moliné-Velázquez et al., 2011; Moliné-Velázquez et al., 2014). For T cell isolation, the splenocytes were resuspended in sorting buffer (sterile 1× PBS with 10% FBS, 25 mM HEPES and 2% P/S:

Gibco) and the Fc receptors were blocked with anti-CD16/CD32 antibodies (Table 1; BD Biosciences) for 10 min at 4 °C. After blocking, Pacific Blue conjugated hamster anti-mouse CD3 (BD Bioscience, for T lymphocyte isolation) or FITC conjugated rat anti-mouse Ly-6C, R-PE conjugated rat anti-mouse Ly-6G and PErCP-Cy5.5 conjugated rat anti-mouse CD11b (BD Biosciences, for MDSC isolation) antibodies were added to the cell suspension and incubated for 30 min at 4 °C in the dark (Table 1). The splenocytes were then washed twice with sorting buffer, recovered by centrifugation at 1500 rpm for 5 min at RT and sorted in a fluorescence activated FACSAria cell sorter (BD Bioscience) located at the Flow Cytometry Service of the *Hospital Nacional de Parapléjicos*. T cells ($CD3^+$ cells) and MDSCs ($Ly\text{-}6C^{high}Ly\text{-}6G^{-/low}$ gated $CD11b^+$ cells) were selected and recovered at a purity > 95%.

2.6. FN-β treatment of Ly-$6C^{high}$-cells/MDSCs alone or in co-culture with T lymphocytes or splenocytes

For T cell activation, flat bottom 96-well plates were coated with purified anti-CD3e/CD28 antibodies (1 μg/ml each; BD Biosciences) for 3 h at 37 °C. Purified $CD3^+$ T cells (2×10^5/well) were plated in RPMI medium (Gibco) supplemented with 10% FBS, 25 mM HEPES, 1% L-glutamine, 1% P/S (Gibco) and 50 μM 2-ME (Sigma), and stimulated for 14 h with anti-CD3e/CD28 (or culture medium alone for the unstimulated controls). Isolated MDSCs were resuspended in IMDM medium (BioWest, Nuaillé, France) supplemented with 2 mM L-glutamine, 1% P/S, 10% FBS (Gibco) and 50 μM 2-ME (Sigma), plated in flat bottom 96-well plates at a density of 5×10^4 (1:4, MDSCs:T cells) or 2×10^4 (1:10), and stimulated with IFN-β (1,000 U/ml) or saline serum for 6 or 18 h. Subsequently, the culture medium was removed and T cells (or fresh medium in the case of culture of MDSCs alone) were added for a further 48 h. The cells were harvested at different time points (0, 6, 18 and 72 h) by centrifugation at 2000 rpm at RT, washed in 1× PBS and analyzed for either myeloid (CD11b, CD11c, MHC-II, F4/80, Ly-6C and Ly-6G: Table 1) markers or process for cell viability analysis. In this case, cells were fixed in 70% ethanol at −20 °C, and stained the following day with a propidium iodide/RNase solution (Immunostep, Salamanca, Spain) according to the manufacturer's instructions. The cells were then analyzed in a FACS Canto II cytometer with FACS Diva 6.1 software, recording 30,000 events.

For MOG-induced stimulation, splenocytes were obtained from MOG-immunized C57BL/6 mice at the peak of clinical score (≥3), as described previously (Moliné-Velázquez et al., 2011; Moliné-Velázquez et al., 2014) and were plated in IMDM (BioWest, Nuaillé, France) supplemented with 2 mM L-glutamine, 1% P/S, 10% FBS (Gibco) and 50 μM 2-ME (Sigma), plated in U-bottom 96-well plates at a density of 2×10^5. Splenocytes were exposed to 5 μM Tag-it Violet™ Proliferation and Cell Tracking Dye (Biolegend) diluted in PBS supplemented with 0.1% BSA at 37 °C for 20 min protected from light. After washing, splenocytes were stimulated for 18 h with 5 μg/mL MOG (or culture medium alone for the unstimulated controls). Isolated Ly-$6C^{high}$-cells/MDSCs were resuspended in IMDM medium (BioWest, Nuaillé, France) supplemented with 2 mM L-glutamine, 1% P/S, 10% FBS (Gibco) and 50 μM 2-ME (Sigma), plated in U-bottom 96-well plates at a density of 5×10^4 (1:4, MDSCs:splenocytes) and stimulated with IFN-β (1,000 U/ml) or saline serum for 18 h (in presence/absence of 5 μg/ml MOG in the case of Ly-$6C^{high}$-cells). Subsequently, the culture medium was removed and splenocytes (or fresh medium in the case of culture of Ly-$6C^{high}$-cells/MDSCs alone) were added for further 48 h. After that, cells were harvested by centrifugation at 1500 rpm at RT, washed in 1× PBS stained with PErCP-Cy5.5-conjugated rat anti-mouse CD11b and APC conjugated hamster anti-mouse CD3 (BD Bioscience) and fixed with 0.1% PFA. At least, 30,000 events were acquired in FACS Canto II flow cytometer (Becton Dickinson, USA) and analyzed with the FacsDiva software (Becton Dickinson, USA).

2.7. In vitro analysis of the immunosuppressive activity of MDSCs from IFN-ß treated mice

To analyze the immunosuppressive activity of MDSCs from IFN-ß treated animals, a different set of EAE mice with a clinical score ranging from 0.5 to 1.5 were injected intraperitoneally with 10,000 units of recombinant murine IFN-β (EAE-IFN-β) or saline (EAE-Veh). The mice were sacrificed three days later and their spleen was dissected out for MDSC extraction by FACS. Sorted MDSCs were immediately plated over control/activated $CD3^+$ T cells (see above), cultured at a density of 2×10^5 cells per well for 24 h at a ratio of 1:4 (MDSCs:T cells) and 48 h later, they were collected and analyzed for myeloid (CD11b, CD11c, MHC-II, F4/80, Ly-6C and Ly-6G) or cell viability staining, as described previously.

2.8. Statistical analysis

The data are expressed as the mean ± SEM and they were analyzed with SigmaPlot version 11.0 (Systat Software, San Jose, CA, USA). Student's *t*-test was used to compare pairs of the different groups of mice and cell cultures, or using a Mann-Whitney U test for non-parametric data, and one way *ANOVA* test was used for multiple comparisons. Pearson's product was obtained for the correlation analyses. Minimal statistical significance was set at $p < .05$: * or # $p < .05$; ** $p < .01$; *** or ### $p < .001$.

3. Results

3.1. The peripheral and CNS MDSCs augments after a single injection of IFN-ß

It is known that the treatment with IFN-ß eases the clinical course of EAE mice (Cheng et al., 2015). Here, a single injection of IFN-β when these animals showed a clinical score between 0.5 and 1.5 significantly reduced the clinical score of the animals from the first day post injection until the peak maximal disability of the EAE-Veh animals (Fig. 1A). To explore whether this effect may be related to MDSCs, we examined the peripheral immune system, *i.e.* principally the spleen (Fig. 1B–E). There was no difference in the global number of splenocytes between treated or vehicle-administered (control) mice (Fig. 1B), or in the total number of myeloid cells per spleen (Fig. 1C–E). By contrast, the percentage of MDSCs within the myeloid subset ($Ly6C^{high}Ly6G^{-/low}$ cells, gated on CD11b) of EAE-IFN-β mice was significantly higher (9.6 ± 1.0, n = 7) than in the control mice (6.7 ± 0.5, n = 4, $p < .05$: Fig. 1D–E). The rest of the myeloid cell types analyzed were not significantly different in the EAE-IFN-β mice: $CD11b^+Ly\text{-}6C^{int}Ly\text{-}6G^{high}$-neutrophils/PMN-MDSCs; $CD11b^+F4/80^+$-macrophages; $CD11b^+CD11c^+$-dendritic cells. Conversely, although the global number of T cells did not change between Veh- or IFN-β-administered mice (Fig. 2A), the proportion of $CD3^+$ T cells was significantly lower after the treatment (vehicle: 27.5 ± 3.1, n = 4; IFN-β: 19.9 ± 1.5, n = 7, $p < .05$: Fig. 2B–C), without affecting their activity state (Fig. 2D–E). These data reinforced the idea of MDSCs as endogenous modulators of the lymphocyte populations, consistent with the strong inverse correlation between the MDSC and T cell component (Fig. 2F). Moreover, IFNAR1, the most common receptor for Type I IFNs (α/β: (Pogue et al., 2004; Schreiber, 2017), was present in half of the splenic $CD11b^+Ly\text{-}6C^{high}Ly\text{-}6G^{-/low}$ cells from EAE mice with a clinical score between 0.5 and 1.5 (when *in vivo* treatments were administered), the same proportion as T cells but more than the global myeloid subset or neutrophils (Fig. 3A–B). Comparing both $CD11b^+Ly\text{-}6C^{high}Ly\text{-}6G^{-/low}$ and T cells, the MFI for IFNAR1 was clearly higher in the former (Fig. 3C).

As the clinical symptoms in this animal model are due to the demyelinating lesions in the CNS, we looked for MDSCs in the spinal cord, their other site of action (Moliné-Velázquez et al., 2011; Moliné-

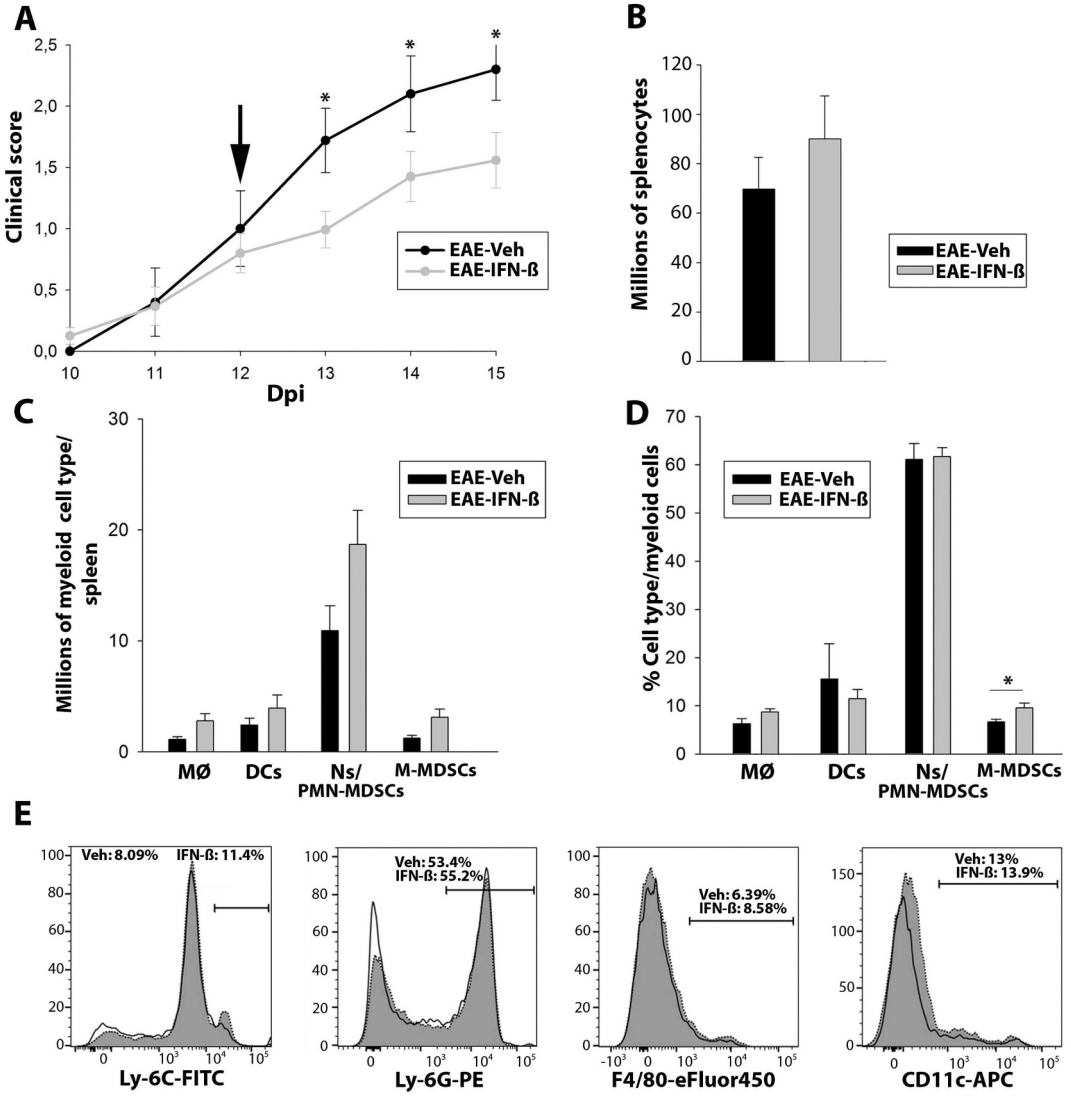

Fig. 1. The MDSC content in the spleen increases after IFN-ß treatment. A: A single injection of IFN-β ameliorates the clinical course of EAE. B: Three days after IFN-β injection, there were no differences in the spleen sizes of both groups. C-D: An analysis of the spleen showed that the global number of myeloid or T cells was not affected by IFN-β. E-F: The percentage of M-MDSCs in the myeloid subset ($CD11b^+Ly\text{-}6C^{high}Ly\text{-}6G^{-/low}$) increased in parallel to a decrease in the proportion of T cells ($CD3^+$) in the spleen after IFN-β treatment. The content of the other myeloid subsets was not modified by this treatment. Black bars refer to the EAE-Veh group whereas the grey bars refer to the EAE-IFN-β group for B to F. G-H: The splenic content of $CD3^+$ T cells was inversely correlated to the percentage of M-MDSCs, normalized to the myeloid component (G) but not relative to the total number of splenocytes (H). Black points represent the EAE-Veh group whereas grey points represent the EAE-IFN-β group. I: Representative examples of flow cytometry plots for each of the splenic cell subsets represented in B (for CD3-PB: white area = EAE-Veh; grey area = EAE-IFN-β; for the rest of plots: continuous line = EAE-Veh; dashed line = EAE-IFN-β) Abbreviations: DCs, dendritic cells; dpi, days post immunization; MØ, macrophages. EAE-Veh n = 4; EAE-IFN-β n = 7.

Velázquez et al., 2014). An initial analysis indicated that the injured area in the EAE-IFN-β animals (7581 ± 1797 μm^2) was significantly smaller than in the EAE-Veh controls (13,561 ± 2,042 μm^2; $p < .05$), and the infiltrated area was mostly confined to the ventral tracts and not infiltration was evident dorsolaterally (Fig. 4A–B). As shown previously, Arg-I can be considered as a marker of MDSCs in the spinal cord of EAE mice at the peak of the disease (Moliné-Velázquez et al., 2011; Moliné-Velázquez et al., 2014). Interestingly, while both control and EAE-IFN-β mice had Arg-I^+ cells in their lesions, they were more evident after IFN-β treatment (Fig. 4A-E). In fact, the significant inverse correlation observed in control mice between the infiltrated area and the density of Arg-I^+ cells was even stronger after IFN-β treatment (EAE-Veh: $r = -0.314$; $p < .01$; EAE-IFN-β: $r = -0.642$; $p < .00001$; Fig. 4F). Together, these data point to MDSC enrichment in both the peripheral immune system and the target tissue (*i.e.*: the CNS) after a single-dose of IFN-ß.

3.2. MDSCs are enriched in the spinal cord myeloid infiltrate of IFN-β treated EAE mice

In order to check whether the phenotype and/or the function of MDSCs were modified after IFN-β treatment, we analyzed the different phenotypes and the activity-associated markers present in these cells: CD11b, Gr-1 and CD124 (IL-4Rα). CD11b is the most common marker of differentiation at the surface of myeloid cells, including MDSCs (Zhu et al., 2007). Among the $CD11b^+$-cells, we discriminated between two distinct populations, $CD11b^+$Arg-I^- and $CD11b^+$Arg-I^+ cells, the latter representing the immunosuppressive subset of MDSCs (Moliné-Velázquez et al., 2011; Moliné-Velázquez et al., 2014). As in EAE-Veh mice, all Arg-I^+ cells expressed the CD11b myeloid marker after IFN-β administration (Fig. 5A–L). However, the composition of the whole myeloid component in the EAE-IFN-β mice was strikingly different from the EAE-Veh control mice. Whereas in EAE-Veh animals the density of

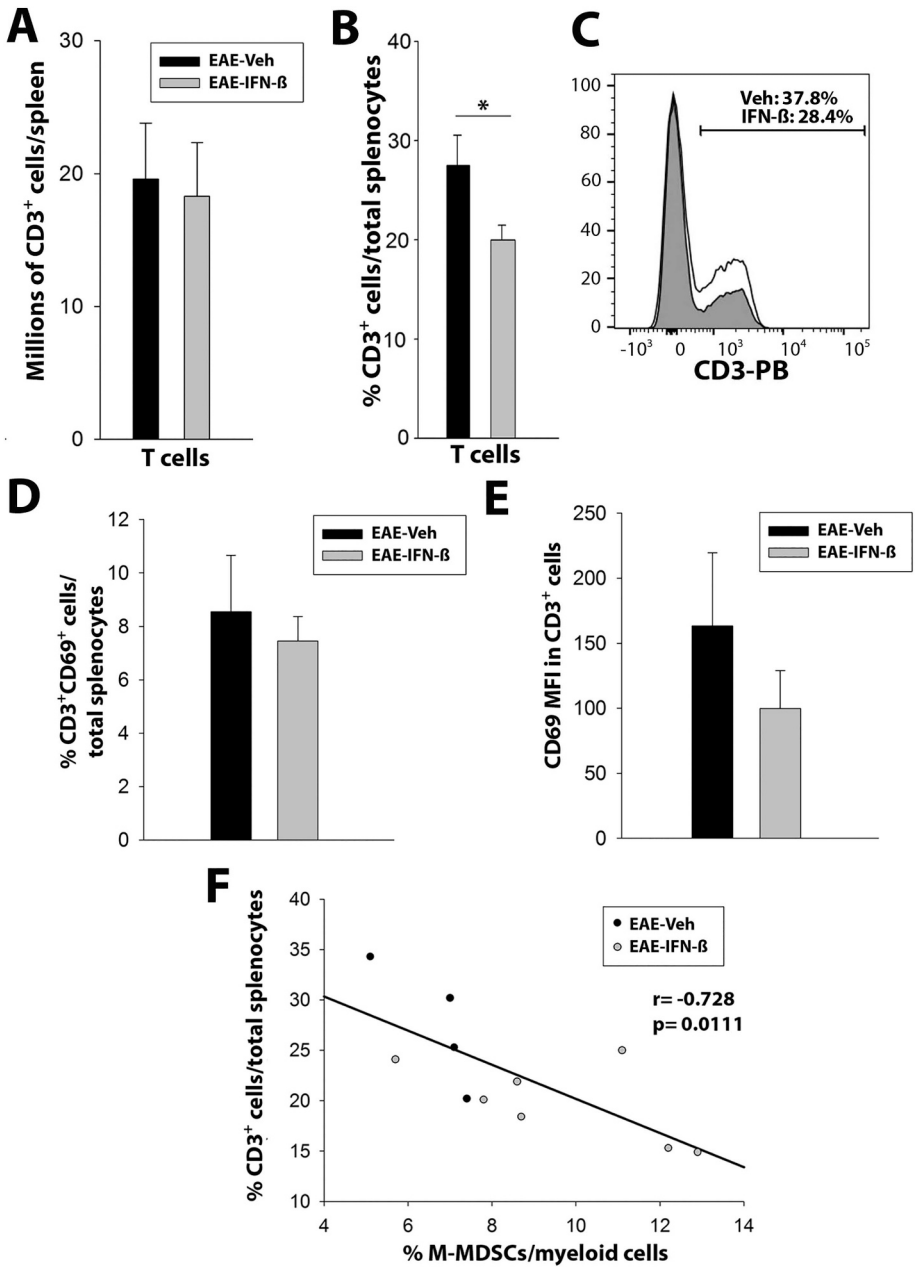

Fig. 2. The T cell population is decreased after IFN-β treatment. A-C: The number of T cells is decreased, both in absolute numbers (A) and relative percentages (B), in the group of EAE-IFN-β compared to the EAE-Veh. This decreased in represented in a plot in C. D-E: The level of activation of the T cells is decreased in the IFN-β-treated mice, as assessed by the percentage and level of intensity of the CD69 marker. However, this decrease is not statistically significant. F: The decrease in the T cell population is inversely related to the amount of MDSCs when referred to the myeloid component. EAE-Veh n = 4; EAE-IFN-β n = 7.

both populations within the infiltrated area was similar, in the EAE-IFN-β mice the density of the dual-labeled cells was about double that of the $CD11b^+Arg\text{-}I^-$ cells ($CD11b^+Arg\text{-}I^-$: vehicle 6,744.0 ± 1,163.5; IFN-β 7,590.4 ± 762.8; $CD11b^+Arg\text{-}I^+$: vehicle 6,720.3 ± 561.8; IFN-β 15,079.7, ± 762.8, $p < .05$ relative to the controls: Fig. 5M). This change in density paralleled a decrease in the proportions of $CD11b^+Arg\text{-}I^-$ cells and an increase in $CD11b^+Arg\text{-}I^+$ cells following IFN-β treatment. This indicated an enrichment of Arg-I^+-MDSCs within the $CD11b^+$ myeloid population (Fig. 5N).

To further analyze the phenotype of the $CD11b^+Arg\text{-}I^+$ subset, we assessed the surface expression of two useful markers of MDSC activity, namely Gr-1 and CD124 (Gallina et al., 2006). As for CD11b, all Arg-I^+ cells within the infiltrated area had faint Gr-1 immunoreactivity (Fig. 6A–F), which has been associated with a stronger capacity of MDSCs to suppress T cells (Moliné-Velázquez et al., 2014; Zhu et al., 2007). Interestingly, we detected a significant decrease in the Gr-1 immunolabelling of Arg-I^+ cells within the CNS of EAE-IFN-ß mice relative to the EAE-Veh mice (IFN-ß: 26.8 ± 1.1; vehicle: 34.1 ± 1.6, $p < .001$: Fig. 6G). CD124 is also an indicator of the higher capacity of MDSC immunosuppression in cancer (Gallina et al., 2006; Kohanbash et al., 2013; Yang et al., 2006) and EAE (Moliné-Velázquez et al., 2014). Although all Arg-I^+ cells were immunostained for CD124 (Fig. 6H-M), it was more intense in the cells from EAE-IFN-β cells (61.3 ± 2.0), than in the cells from the EAE-Veh mice (43.1 ± 1.8; $p < .001$: Fig. 6N). In order to check whether this change in the immunosuppressive phenotype can have a parallel on MDSC activity over T cells, double labeling of MHC-II and PD-L1 were carried out in Arg-I^+ cells. MDSCs have been ascribed a poor antigen presenting capacity (Gabrilovich et al., 2012; Zhu et al., 2011). Interestingly, we detected a significant decrease in the percentage and MFI ratio of MHC-II immunolabelling of Arg-I^+ cells

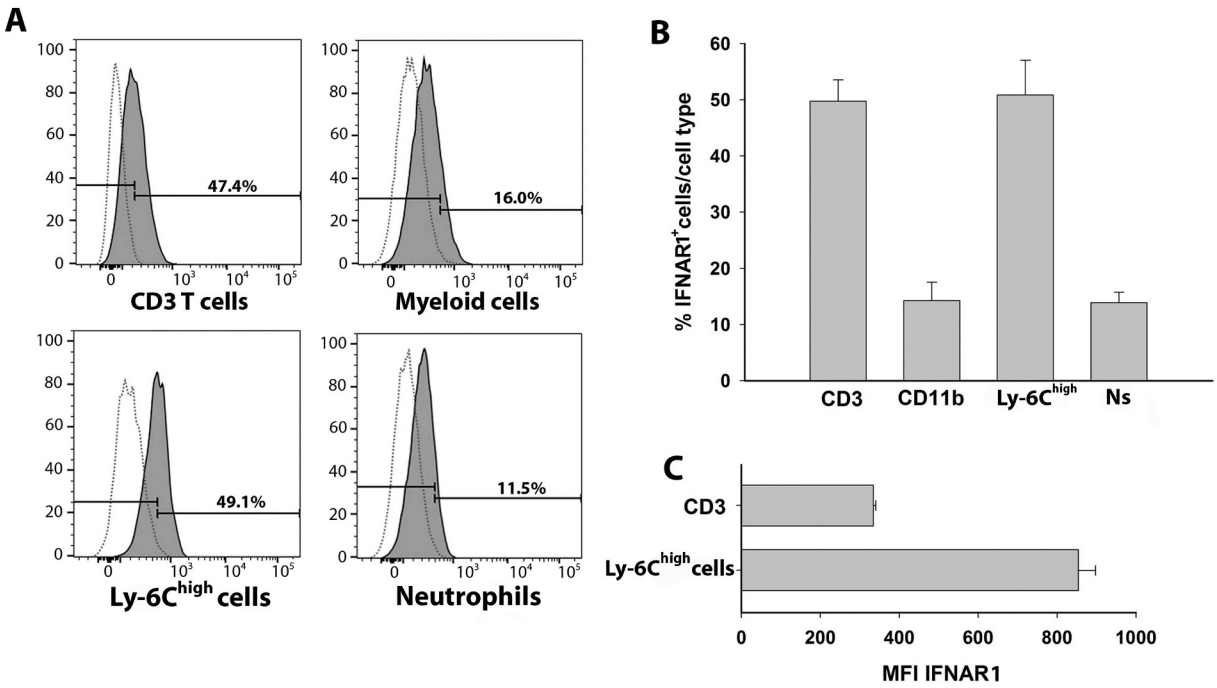

Fig. 3. IFNAR is mainly present in splenic Ly-6C^{high} cells at the time of IFN-β injection. A: Representative plots of the cells containing IFNAR1 in the spleen, as represented in B (clinical score 0.5–1.5). B: T cells and Ly-6C^{high} were the two cell subsets with most IFNAR containing cells in the spleens analyzed. C: Ly-6C^{high} presented a higher IFNAR1 MFI than CD3$^+$ T cells (n = 3).

within the CNS of EAE-IFN-β mice when compared to the EAE-Veh mice (percentage: IFN-β: 42.1 ± 1.9; vehicle: 67.5 ± 5.2, p < .05; MFI: IFN-β: 20.7 ± 3.6; vehicle: 35.0 ± 5.3, p < .05; Fig. 7A-H). Moreover, the PD-L1 pathway in myeloid cells has been shown to be crucial for EAE control regulation in a strain specific manner (Salama et al., 2003; Zhu et al., 2006) and MDSCs have been demonstrated to present a PD-L1$^+$ profile (Casacuberta-Serra et al., 2016). Remarkably, after IFN-β treatment, the percentage of MDSCs with PD-L1 immunolabelling was significantly higher without affecting the MFI of PD-L1 in Arg-I$^+$ cells within the CNS relative to the EAE-Veh mice (percentage: IFN-β: 54.8 ± 1.8; vehicle 40.1 ± 1.7, p < .001; MFI: IFN-β: 61.8 ± 2.7; vehicle: 64.7 ± 2.0, p = .404: Fig. 7I–O). This acquisition of a more suppressive phenotype was accompanied by an increase in the density of TUNEL$^+$CD4$^+$ T cells within the infiltrated areas of the spinal cord (vehicle: 514.0 ± 79.3; IFN-β: 1,501.3 ± 438.7, p < .05: Fig. 8A–G).

Together these data strongly suggest that the immunosuppressive phenotype of MDSCs is promoted after a single dose of IFN-ß within the CNS of EAE mice.

3.3. MDSCs present a promoted T cell suppressive activity after IFN-ß treatment

In order to check whether the modulation of MDSCs towards a stronger suppressive phenotype occurred *in vivo* after IFN-ß administration, we performed an *in vitro* assay with MDSCs obtained from EAE-Veh or EAE-IFN-β mice. EAE mice with a clinical score ranging 0.5 to 1.5 received a single injection of IFN-β (10,000 units) or the vehicle alone, and their spleen was removed three days later. MDSCs isolated from the EAE mice that received saline (MDSC-Veh) or IFN-β (MDSC-IFN-β) were co-cultured for 48 h with control or anti-CD3e/CD28 pre-activated T cells in a 1:4 ratio (MDSC:lymphocytes: Fig. 9A–B). Propidium iodide analysis of cell viability test indicated that MDSC-IFN-β significantly increased the dead (EAE-Veh: 0.5 ± 0.1; EAE-IFN-β: 0.76 ± 0.17, p < .05: Fig. 9B′) or apoptotic T cells (EAE-Veh: 17.3 ± 2.5; EAE-IFN-β: 25.0 ± 3.0, p < .05: Fig. 9B″), in conjunction with a significant reduction in the proportion of viable T cells (EAE-Veh: 82.2 ± 2.5; EAE-IFN-β: 74.2 ± 3.2, p < .05: Fig. 9B‴). Interestingly, there were no changes in the dead, apoptotic or viable control T cells when they were exposed to MDSC-Veh or MDSC-IFN-β (Fig. 9B). In conclusion, MDSCs from mice that were administered IFN-β were not only more abundant but they also had a stronger *in vitro* immunosuppressive effect over activated T cells.

In order to check whether the potentiation of the immunosuppressive role of MDSCs at the peak might be related to a specific role of IFN-β at the therapeutic window for its administration, splenic Ly-6C^{high}-cells isolated at the onset of the EAE course (clinical score 0.5–1.5) were pre-treated with saline (Ly-6C^{high}-Veh) or IFN-β (Ly-6C^{high}-IFN-β) during 18 h either in the presence or absence of 5 μg/ml MOG. Subsequently, the Ly-6C^{high}-cells were co-cultured with 5 μg/mL MOG pre-activated splenocytes from EAE mice at the peak of the clinical course in a proportion of 1:4 (MDSCs:splenocytes), and cell proliferation was assessed (Fig. 9C). The Ly-6C^{high}-Veh provoked significantly stronger proliferation in MOG-activated T cells than in the splenocytes alone, which was abrogated in presence of Ly-6C^{high}-IFN-ß (Proliferation index: Stimulated splenocytes alone: 6.1 ± 0.6; Ly-6C^{high}-Veh 10.5 ± 2.5; Ly-6C^{high}-IFN-ß: 7.9 ± 1.0; Fig. 9D). Remarkably, this effect was independent of the pre-exposition of Ly-6C^{high}-cells to MOG (Ly-6C^{high}-Veh + MOG: 8.8 ± 0.8; Ly-6C^{high}-IFN-ß + MOG: 7.3 ± 0.8). These data indicate that the pro-inflammatory effect of Ly-6C^{high}-cells at the onset of the disease can be blocked, or at least, reduced, in presence of IFN- ß.

In order to determine if this enhanced immunosuppression could also be induced *in vitro*, we designed an assay in which MDSCs extracted from EAE mice at the peak of their disability were pre-treated with saline (MDSC-Veh) or IFN-ß (MDSC-IFN-ß) for 18 h prior to co-culture. Subsequently, the MDSCs were co-cultured with either control, anti-CD3e/CD28 activated CD3$^+$ T cells from control mice or MOG-pre-activated splenocytes from EAE mice at the peak of the disease in a proportion of 1 MDSC:4 T cells/splenocytes), and cell viability or a proliferation assay was assessed (Fig. 10A, D). The MDSCs-IFN-ß provoked significantly stronger cell death (MDSCs-Veh: 0.5 ± 0.1; MDSC-IFN-β: 1.6 ± 0.3, p < .01) or apoptosis (MDSC-Veh: 33.6 ± 7.5; MDSC-IFN-β: 55.2 ± 5.0, p < .05) in overactivated T cells than in the control MDSCs, and a significant reduction in the proportion of viable T

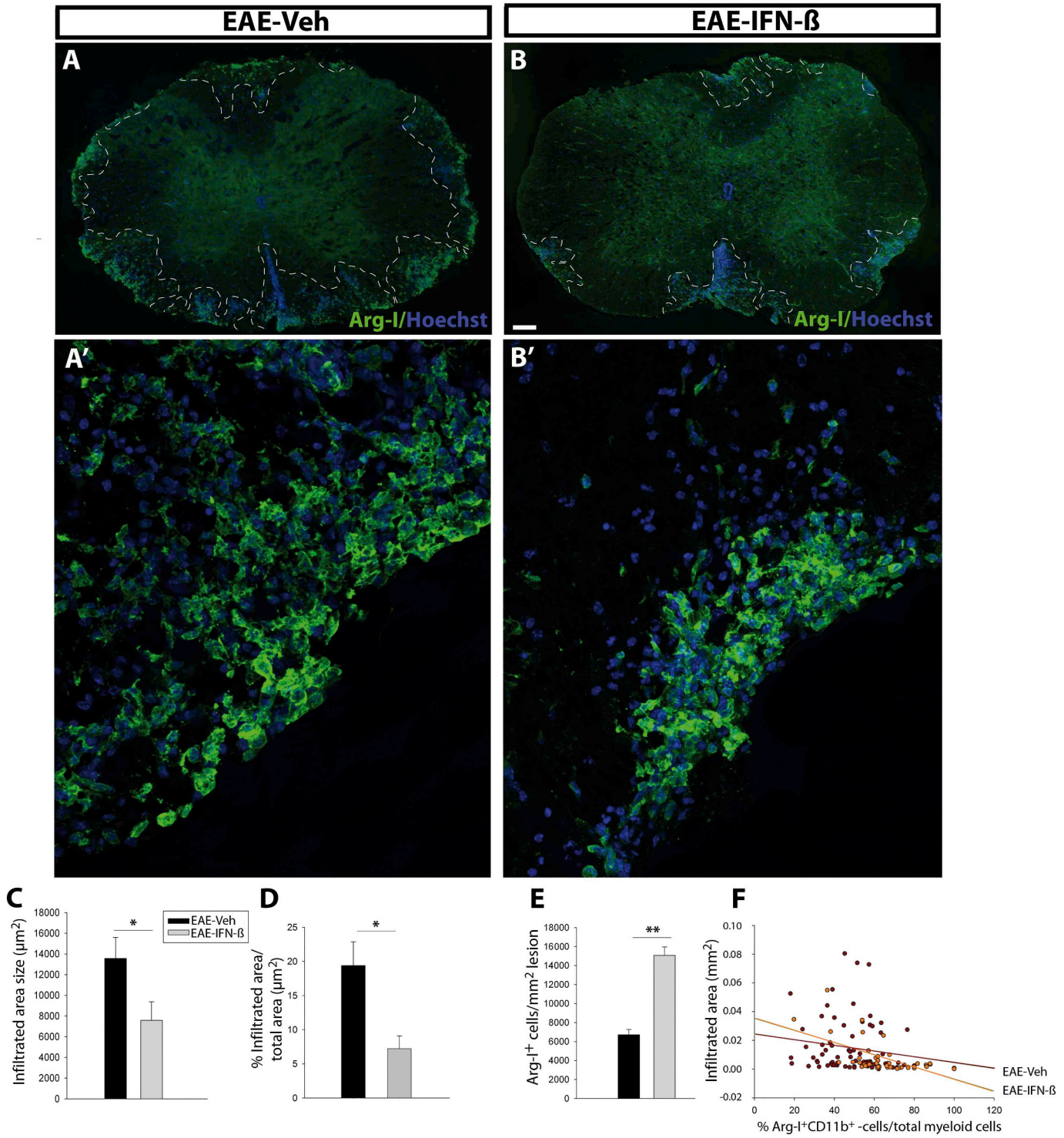

Fig. 4. An enrichment in the Arg-I$^+$ MDSCs within the lesioned area of the spinal cord is present after IFN-β treatment of EAE mice. A-B′: Representative panoramic views of spinal cords of EAE-Veh or EAE-IFN-β mice three days after injection. The dashed lines define the infiltrated area. A′-B′: Detailed views of a representative infiltrated area of the spinal cord of EAE-Veh or EAE-IFN-β mice. C-E: IFN-β injection induced a decrease in both the size of the lesion (C) and in the proportion of the white matter it represented (D). By contrast, the density of Arg-I$^+$ cells increased significantly in EAE-IFN-β compared to EAE-Veh mice (E). F: A significant inverse correlation was found between the Arg-I$^+$ cell content in the spinal cord of each lesion and the lesion size, which was even more pronounced in the EAE-IFN-β animals (EAE-Veh: $r = -0.314$, $p < .01$, EAE-IFN-β: $r = -0.642$, $p < .001$). Red circles represent the EAE-Veh group while yellow circles represent the EAE-IFN-β treated group. Scale bar: A-B = 150 µm; A′-B′ = 25 µm. EAE-Veh n = 4; EAE-IFN-β n = 4. (For interpretation of the references to colour in this figure legend, the reader is referred to the web version of this article.)

cells (MDSC-Veh: 65.9 ± 7.6; MDSC-IFN-β: 42.6 ± 5.1, $p < .05$; Fig. 10B; Supplementary Fig. 1A–C). Remarkably, this effect was only seen on over-activated T cells and not on control T cells, demonstrating the specificity of the effect. When we performed these same assays with a lower proportion of MDSCs (1:10), there appeared to be a similar effect on T lymphocyte cell viability and thus, stronger T cell immunosuppression, although this did not reach significance (Fig. 10C, Supplementary Fig. 1D–F). On the other hand, the proliferation of

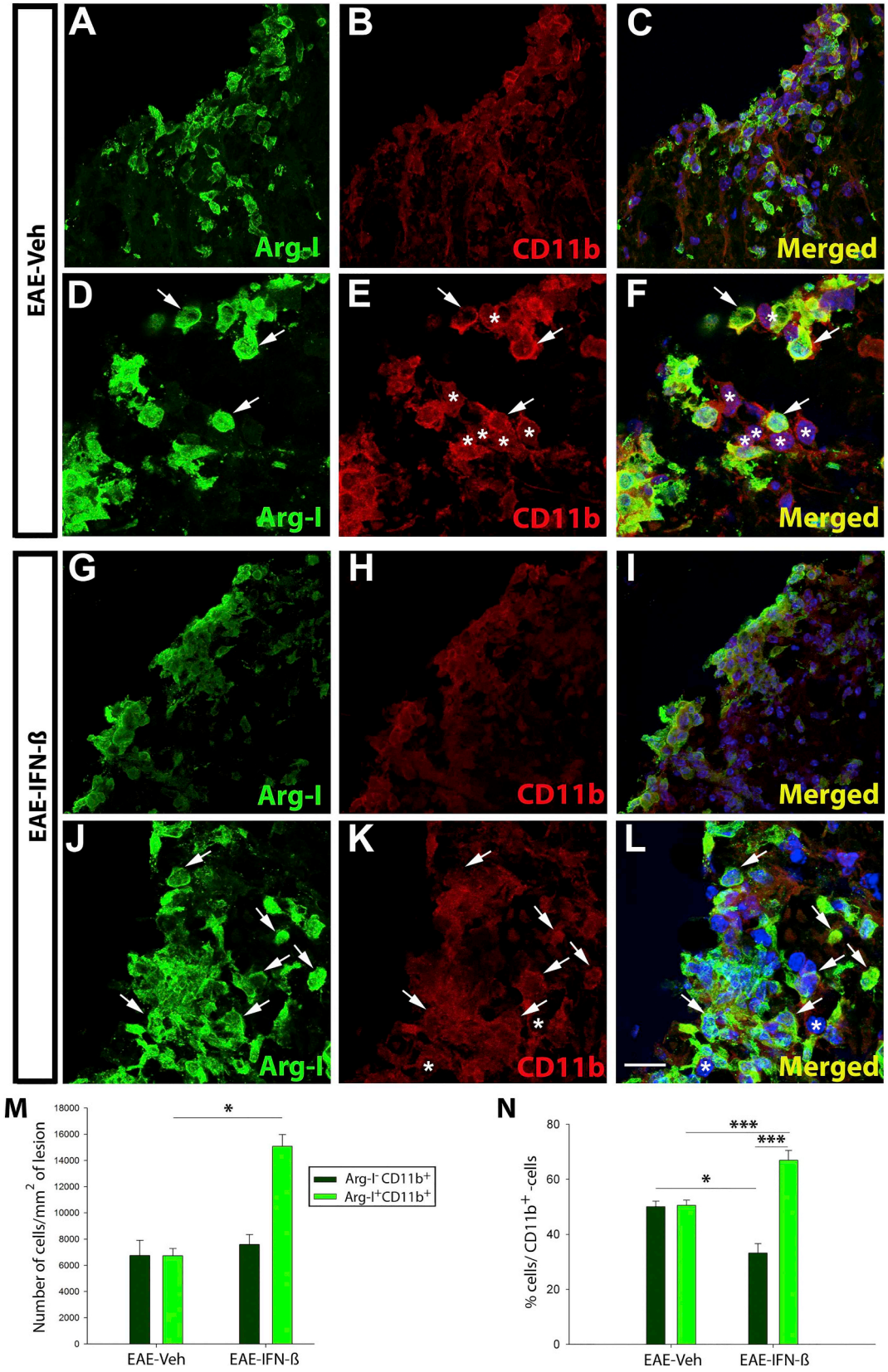

Fig. 5. The myeloid cell subset within the spinal cord of EAE mice is enriched in MDSCs after IFN-β treatment. A-L: Representative panoramic views (A-C and G-I) and detailed images (D-F and J-L) of the infiltrated areas within the spinal cord of EAE-Veh (A-F) or EAE-IFN-β (G-I) mice. Arrows point to double-labeled cells and the asterisks indicate Arg-I^{-}/CD11b^{+} cells. P-Q: The population of Arg-I^{+}/CD11b^{+} MDSCs increases after IFN-β treatment as shown by the significantly higher density of double-labeled cells (P) and the proportion of the whole CD11b^{+}-myeloid cell population they represent (Q). Scale bar: A-C; G-I = 25 μm and D-F; J-L = 10 μm. EAE-Veh n = 4; EAE-IFN-β n = 4.

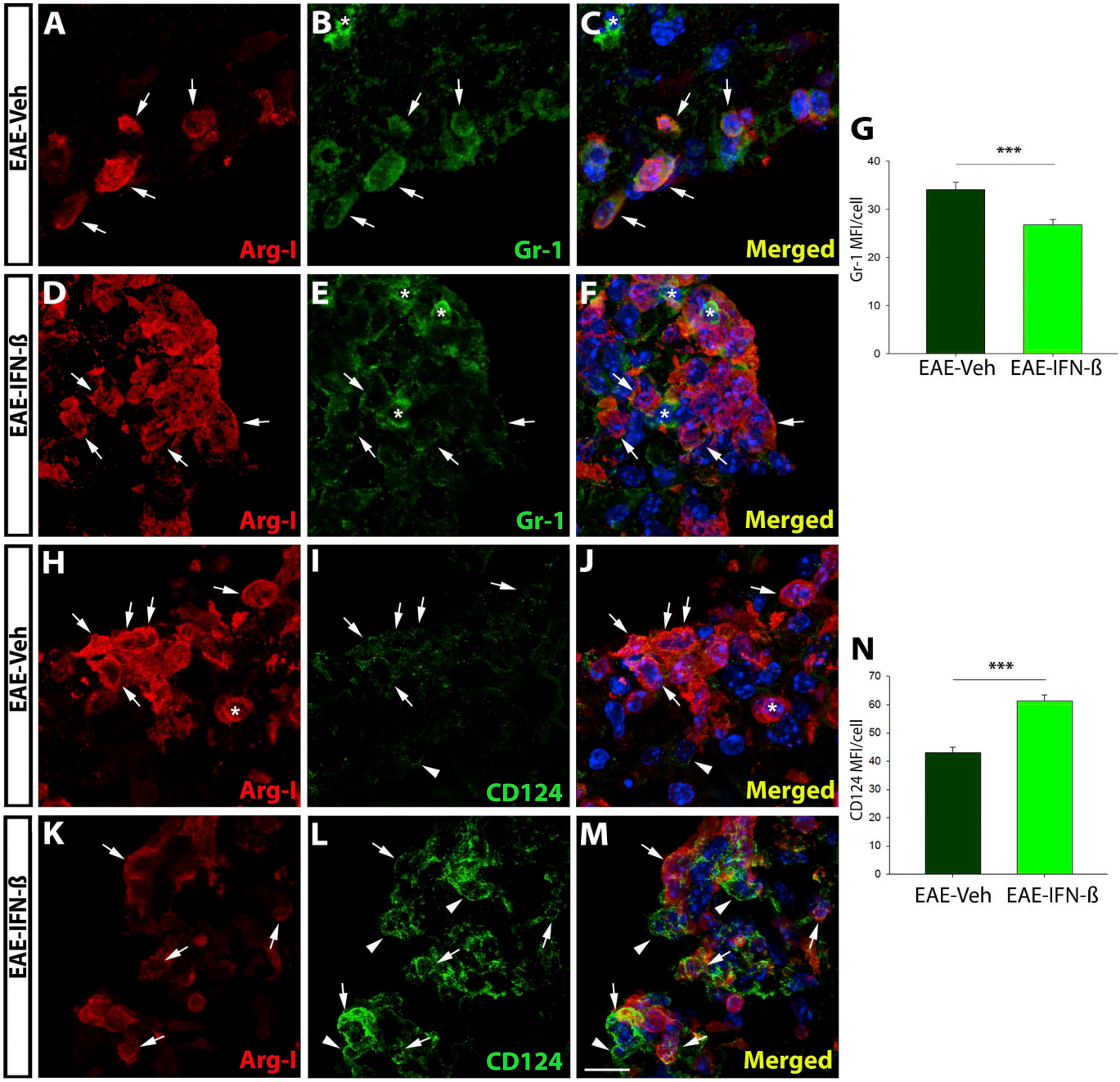

Fig. 6. MDSCs from EAE-IFN-β mice have an enhanced immunosuppressor phenotype in the spinal cord. A-G: Although all Arg-I$^+$-cells are immunostained for Gr-1, this was significantly fainter in EAE-IFN-ß than in EAE-Veh mice. H-N: The staining intensity of CD124 in the Arg-I$^+$ cells increased dramatically after IFN-β treatment. Scale bar: A-F, H-M = 25 μm. EAE-Veh n = 4; EAE-IFN-ß n = 4.

MOG-preactivated T cells was reduced when co-cultured with both MDSC-Veh or MDSC-IFN-ß, being statistically significant in the latter (proliferation index: Stimulated splenocytes alone: 5.7 ± 0.2; MDSCs-Veh: 4.7 ± 0.4, p = .120; MDSC-IFN-β: 4.1, ± 0.4, p < .05; Fig. 10E). Together, these data indicate that MDSCs present a more powerful immunosuppressive effect after IFN-β treatment, which can also be induced *ex vivo*, and that affects to both policlonally activated and encephalitogenic T cells.

3.4. IFN-β maintains MDSC undifferentiated state

To explain the influence of IFN-β on MDSCs and given that the immunosuppressive activity of MDSCs is strongly determined by their state of maturity (Moliné-Velázquez et al., 2014), we carried out a time-course analysis of the main surface marker of M-MDSCs, namely Ly-6C, and of a marker of a mature subset of cells, the macrophage marker F4/80. When we assessed the MFI of Ly-6C after treatment with IFN-ß, the significant loss of Ly-6C MFI after 6 h *in vitro* by MDSCs-Veh was not evident in the MDSC-IFN-ß. However, the Ly-6C MFI did shift in the INF-β treated MDSCs after 18 h *in vitro*, reaching a similar value to those in recently sorted cells (Fig. 11A). In addition, the differentiation of the cultured MDSCs was assessed by measuring their F4/80 expression, a marker of macrophage polarization. MDSC-Veh differentiated during their time in culture to a more mature F4/80 subset, whilst the IFN-ß treated MDSCs express less F4/80 after 18 h *in vitro* (Fig. 11B). All these data indicate that IFN-ß is a potent regulator of the immature MDSC immunosuppressive phenotype.

In order to determine whether INF-β produced a permanent and

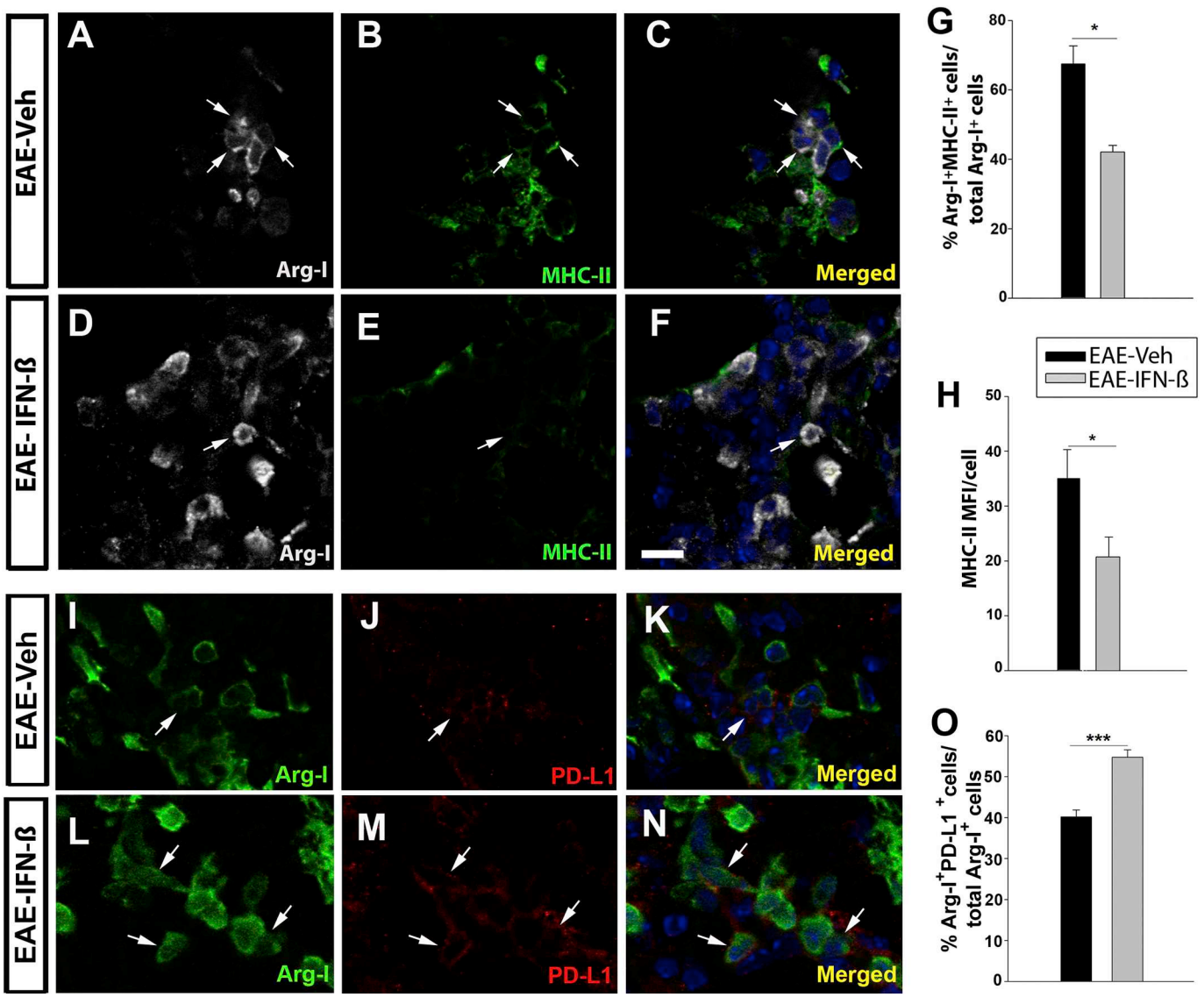

Fig. 7. The spinal cord of EAE mice present a lower content of MDSCs with antigen presenting cell capacity and increased T cell suppressive phenotype after IFN-β treatment. A-F: Inflammatory lesions within the spinal cord of EAE-Veh mice (A-C) and EAE-IFN-β mice (D-F) labeled for Arg-I in white and MHC-II in green. G-H: The lesions from EAE-IFN-ß mice presented a lower Arg-I$^+$MHC-II$^+$ cell content in comparison to the EAE-Veh group (G), exhibiting a down-regulation in their fluoresce intensity for the MHC-II marker (H). I-N: Detailed images of cell infiltrates within the spinal cord of EAE-Veh mice (I-K) and EAE-IFN-ß mice (L-N) labeled for Arg-I in green and PD-L1 in red. O: The percentage of Arg-I$^+$PD-L1$^+$ cells is increased in the group of IFN-ß-treated mice compared to the vehicle-treated mice. Abbreviations: MFI = mean fluorescence intensity. White arrows point to double-labeled cells. Scale bar: A-F; I-N = 10 μm. EAE-Veh n = 4; EAE-IFN-ß n = 4. (For interpretation of the references to colour in this figure legend, the reader is referred to the web version of this article.)

direct effect that preserved MDSCs in an undifferentiated state under the different co-culture conditions used in the immunosuppression experiments, we analyzed the MDSC phenotype (Ly-6C and F4/80 MFI) when cultured alone or together with activated T cells, and we compared it with the phenotype observed at the end of the IFN-β treatment (18 h). An increase in Ly-6C MFI was only stimulated in MDSCs-Veh in the presence of activated T cells (Fig. 11C), whereas IFN-β pre-treatment predisposed MDSCs towards a significantly higher Ly-6C MFI in all culture conditions. In the case of F4/80, the high MFI observed in the MDSCs-Veh after 18 h culture did not vary significantly among the experimental groups. By contrast, the removal of IFN-β from the culture produced a significant increase in the F4/80 MFI when MDSCs were cultured alone or in the presence of unstimulated T cells, while it remained similar to that at the end of the treatment (18 h) when they were cultured together with activated T cells (Fig. 11D). Comparing the MFI of Ly-6C between MDSCs-Veh or MDSCs-IFN-β, the latter always displayed stronger fluorescence than the former, irrespective of the presence or absence of the cytokine (Fig. 11E). In terms of F4/80, the MFI was only weaker at the end of the treatment, while it remained similar in the rest of the conditions, *i.e.* when IFN-β was removed from the culture medium (Fig. 11F). Overall, these data indicated that IFN-β prevented MDSC differentiation when added to the culture medium, exerting a persistent effect on Ly-6C expression, whereas its effect on F4/80 was fully dependent on the presence of this factor.

4. Discussion

In the present work, for the first time we propose that the number and suppressive capacity of MDSCs in the context of EAE is modified after IFN-ß treatment. We show that a single injection of a therapeutic dose of IFN-ß at the onset of the symptoms significantly ameliorates the clinical course of the disease. This effect parallels the increase in the presence of MDSCs in both the spleen and the infiltrated areas of the spinal cord. Moreover, MDSCs isolated from EAE mice administered

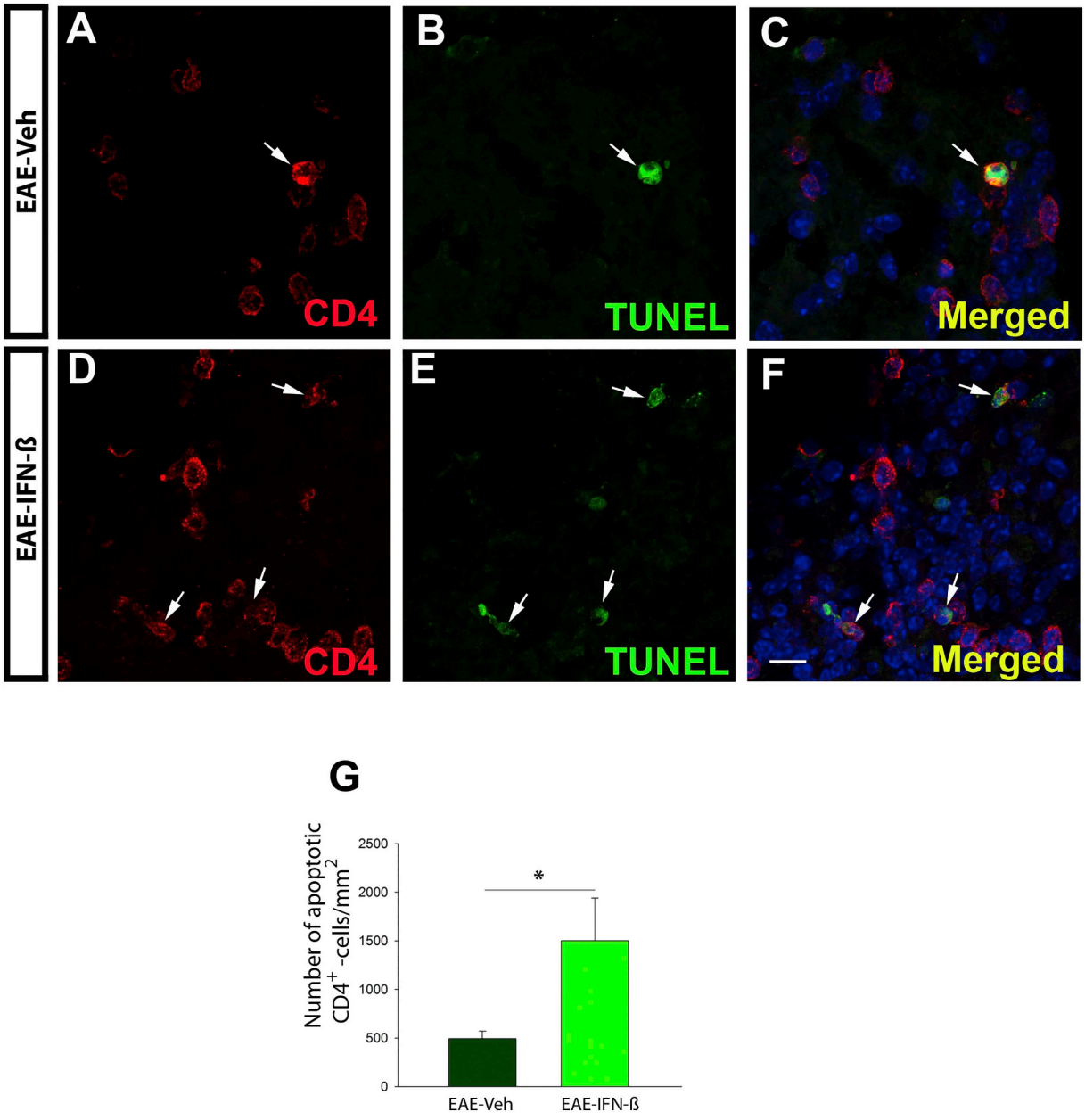

Fig. 8. IFN-ß promotes an increase in $CD4^+$ T cell death in the spinal cord of EAE mice. A-G: The density of apoptotic $CD4^+$ T cells was significantly higher in EAE-IFN-ß mice compared to EAE-Veh animals. Arrows point to $CD4^+TUNEL^+$ cells. Scale bar: A-F = 10 µm. EAE-Veh n = 4; EAE-IFN-ß n = 4.

IFN-β are stronger immunosuppressors, which is consistent with a higher density of apoptotic T cells in the CNS, the main target of this population (Moliné-Velázquez et al., 2011; Zhu et al., 2007). In addition, our *in vitro* studies also demonstrate that IFN-β enhances the immunosuppressive effect of MDSCs on over-activated T cells possibly due to the preservation of their immature state.

Although IFN-β has been shown to ameliorate RRMS by delaying the onset of new relapses, decreasing the severity of the symptoms of relapse, and/or controlling the proliferative response mediated by antigen presenting cells (APCs; Arnason, 2005; Jankovic, 2010), our data show that the enhancement of T cell immunosuppression by MDSCs after IFN-ß administration may also contribute to this effect (Kieseier, 2011). There are two different experimental approaches to demonstrate that the administration of IFN-ß exerts a direct effect onto MDSCs: i) to eliminate/inactivate MDSCs at the onset of the EAE course and subsequently check whether IFN- ß administration still exerts the same effect in absence of MDSCs, or ii) to transplant MDSCs from EAE-IFN-ß treated mice in recipient EAE mice just at the same moment that our therapeutic window, *i.e.* the onset of symptoms during the clinical course. However, due to the extremely high plasticity of the activity state in $CD11b^+Ly\text{-}6C^{high}Ly\text{-}6G^{-/low}$ ($Ly\text{-}6C^{high}$-cells) along the EAE course, both options would bring false negative results. The elimination of $Ly\text{-}6C^{high}$-cells at the onset of the disease (a cell type with an already demonstrated pro-inflammatory profile: Giles et al., 2018; King et al., 2009; Yi et al., 2012; Zhu et al., 2011) would ameliorate EAE clinical course by itself. On the other hand, the transplantation of MDSCs isolated at the peak of the disease, a moment when the molecular environment drive myeloid-infiltrating cells towards a clear anti-inflammatory activity state (Giles et al., 2018), into EAE mice at the onset of their disease (a clinical moment with a prominent pro-inflammatory environment), may be a risk for a successful clinical course amelioration. Indeed, it has been shown that induced-MDSCs transplanted at the onset of the EAE clinical course do not result in a less severe disease course (Casacuberta-Serra et al., 2016). In our hands, although still

indirect, the higher suppressive activity of MDSCs isolated from IFN-ß-treated mice, together with the abrogated proliferative promotion of Ly-6C^{high}-cells isolated at the onset of the disease over MOG-stimulated splenocytes, suggest a direct effect of IFN- ß modifying the activity state of this plastic cell type, from purely pro-inflammatory to clearly anti-inflammatory.

Indeed, different myeloid subsets infiltrating the CNS may respond to IFN-β in EAE, as is the case of blood and bone marrow derived macrophages and dendritic cells (Wlodarczyk et al., 2015). Our data show that splenic Ly-6C^{high} cells express IFNAR1 more strongly than the

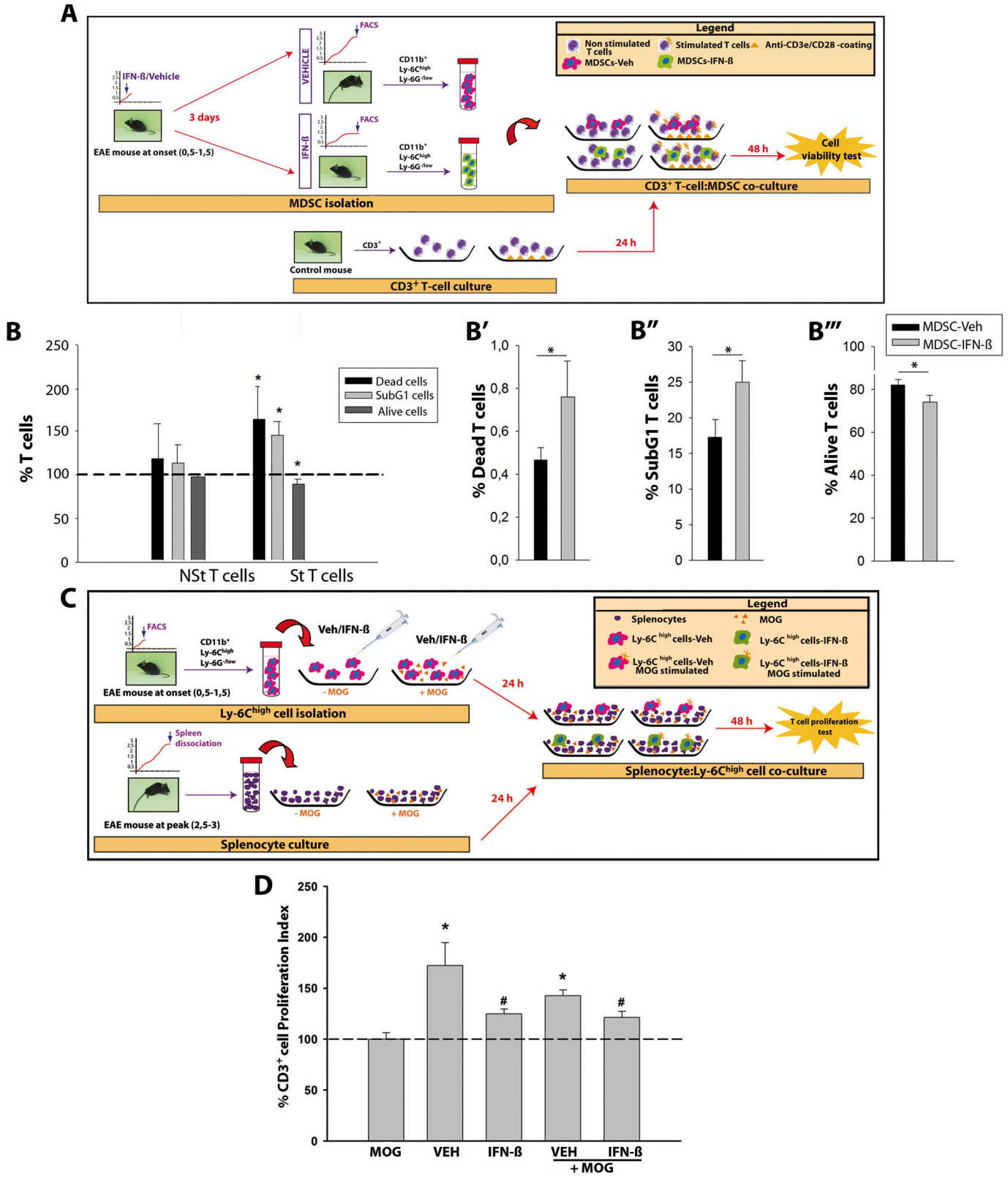

(caption on next page)

Fig. 9. The immunosuppressive capacity of MDSCs is enhanced after IFN-ß treatment. A. Schematic representation of the experimental procedure quantified in B. EAE mice were administered saline or IFN-β when they had reached a clinical score between 0.5 and 1.5. Three days later, their spleens were dissected out, and MDSCs were isolated by cell sorting and exposed to control or to anti-CD3e/CD28 stimulated T cells sorted from non-immunized mice. B-B‴. Analysis of cell viability in the different co-cultures. Bars represent the percentage of non-viable (dead and apoptotic cells) and viable T cells in co-culture with MDSCs-IFN-ß or MDSCs-Veh (dashed line). MDSCs–IFN-ß had a significantly stronger suppressive activity than MDSCs-Veh when co-cultured with T cells stimulated polyclonally. This effect was not observed when they were in contact with unstimulated T cells. B′-B‴: Representation of the absolute percentages of the non-viable and viable stimulated T cells in contact with MDSC-Veh or MDSCs-IFN-ß. C: Layout of the co-culture of Ly-6C^{high}-cells isolated at the onset of the EAE (0.5–1.5 of clinical score) and splenocytes from EAE mice at the peak of the disease (clinical score ≥ 3.0). D. Histogram showing that Ly-6C^{high}-cells isolated at the onset of the disease promoted the proliferation of T cells, which was dampened when they were pretreated with IFN-ß. Besides, the presence of MOG in the culture of Ly-6C^{high}-cells did not affect to this biological effect. Asterisks represent the statistical significance compared to the dashed line, and hashes compared to the respective vehicle group. n = 3/group in A-B, n = 5/group in C-D.

general myeloid cell subset or neutrophils, and even more so than T cells, an immune cell type with particularly strong expression of this receptor (Kavrochorianou et al., 2016). Different IFNAR-containing cell types were analyzed in gene-targeted mice to reveal the cell target of IFN-β in EAE during the effector phase of the model, including resident CNS cells, lymphocytes and myeloid cells (Prinz et al., 2008). Myeloid cells are important for EAE disease progression, especially CD11b$^+$Ly-6C$^+$ cells. Regarding MHC-II$^+$-APCs, IFN-ß downregulates myelin uptake by macrophages (Prinz et al., 2008), reducing the antigen-presenting capacity of microglial cells (Teige et al., 2006) and promoting the switch of M1 to M2 microglia (Tarassishin et al., 2011). All these data point to IFNAR-expressing Ly-6C^{high} myeloid cells as one of the main targets for IFN-ß during immune-mediated demyelination.

Although IFN-ß has different effects on T cell biology during EAE and MS (Galligan et al., 2010; Teige et al., 2006; Trinschek et al., 2015; Rudick et al., 1993), our current data demonstrate for the first time that the decrease in T cell activity mediated by IFN-β may also be indirectly due to the improvement of highly specialized immunosuppressive agents, *e.g.*, MDSCs. Indeed, for several decades it has been known that IFN-ß production is a common feature of natural suppressor agents, a compilation of cell types/mechanisms that inhibit both the activity and proliferation of T cells in a non-MHC restricted manner (Cleveland et al., 1988). In this respect, it was recently shown that IFN-ß therapy in MS patients regulates the responsiveness of activated T cells to the immunosuppression mediated by Tregs (Trinschek et al., 2015), cells that are induced by MDSCs in different pathological scenarios (Melero-Jerez et al., 2016). Furthermore, IFN-ß has been demonstrated *in vitro* to be critical for the NO-mediated enhancement of the suppressor activity of CD31$^+$CD11b$^+$Ly-6C$^+$Ly-6G$^+$ immature myeloid cells isolated from bone marrow-derived cells (Campillo et al., 2006), an immunosuppressive mechanism shared with MDSCs (Melero-Jerez et al., 2016; Moliné-Velázquez et al., 2016).

We have traditionally used Arg-I to label M-MDSCs at the peak of the EAE clinical course. In this sense, all Arg-I$^+$-cells showed immunoreactivity to the main two necessary markers to identify MDSCs by flow cytometry, *i.e.* CD11b and Gr-1. In addition, all Arg-I$^+$-cells showed CD115 immunoreactivity (a good marker to discriminate M-MDSCs) and none of them presented Ly-6B.2 staining (a typical marker for PMN-MDSCs or mature neutrophils). Although several reports have shown that the Arg-I$^+$-cell population within the CNS seemed to be more heterogeneous than it was previously thought (Moliné-Velázquez et al., 2014; Giles et al., 2018), all of them remain CD11b$^+$Gr-1$^+$ independently of the administered treatment (present results; Moliné-Velázquez et al., 2014), showing a CD115$^+$ phenotype (data not shown). After a single injection of IFN-β in the EAE model, there was an accumulation of the Arg-I$^+$-MDSCs with a more potent immunosuppressive phenotype, consistent with the accumulation of splenic Ly-6C$^+$ cells recently described in a mouse model of chronic viral infection (Taleb et al., 2017). Both these effects might be the result of: i) a direct IFN-β mediated action on MDSCs; or ii) the consequence of a more general IFN-β induced anti-inflammatory immunomodulation in both the periphery and CNS. In relation to a possible direct effect, IFN-β influences several aspects of MDSC biology. One of the most important aspects of their immunosuppressive effect is the blockage of their differentiation into mature cells, as normally occurs upon inflammatory insult, and indeed, our data suggests IFN-β impairs MDSC maturation. Although the underlying mechanism remains to be revealed, we present here the first evidence that IFN-ß maintains MDSCs in an undifferentiated state *in vitro*. This is probably related to how IFN-ß engages with its receptor at the cell membrane, as the effect on F4/80 expression is fully dependent on the presence of IFN-ß. In relation to MDSC maturation, the IRF8 transcription factor (Interferon Response Factor 8) is determinant for CD11b$^+$Gr-1$^+$-MDSC accumulation (Scheller et al., 1999; Sonda et al., 2011; Stewart et al., 2009), and a deficiency in IRF8 leads to abnormal hematopoiesis and it abrogates the termination of emergency granulopoiesis (Hu et al., 2016). Such effects are consistent with our *in vitro* results regarding the preservation of MDSC immaturity. However, further *in vivo* experiments will be needed to determine if these are direct effects of IFN-β on MDSCs that are responsible for the amelioration of the clinical course of EAE.

We show an enrichment of CD11b$^+$Arg-1$^+$ MDSCs within the myeloid compartment in the infiltrated CNS following IFN-β treatment, within the already smaller lesions that have higher cellularity than in EAE-Veh mice. This may reflect the enhanced migration/mobilization of MDSCs towards the inflammatory sites. Although the function of Ly-6C in monocytes still remains to be determined, its blockade decreases monocyte infiltration in a mouse model of amyotrophic lateral sclerosis (Butovsky et al., 2012). As we also demonstrated *in vitro*, Ly-6C expression is increased in the presence of IFN-ß and its effect persists for at least 72 h in culture. Ly-6C is a useful membrane antigen to distinguish different subpopulations of mouse blood monocytes as a function of their stage of maturation and their capacity to migrate towards inflammatory sites. Ly-6C is down-regulated in circulating blood under normal conditions but it increases after various inflammatory insults (Sunderkotter et al., 2004). Regarding MDSC migration, the stronger expression of this molecule on monocytes is related to the so-called immature or inflammatory monocytes, *i.e.*: the Ly-6C^{high} monocytes isolated at the disease onset (Saederup et al., 2010). These cells express CCR2 (Serbina and Pamer, 2006), a chemokine receptor absent in Ly-6C^{low} monocytes (mature or resident monocytes), and it is closely related to their capacity to cross the BBB in EAE (Mildner et al., 2009; Saederup et al., 2010). Therefore, the higher Ly-6C MFI in MDSCs after IFN-β treatment may indicate a greater infiltration capacity of these cells, which helps them invade the CNS of EAE mice. Interestingly, the Ly-6C gene is thought to be regulated by IFN-β since it has IFN response elements in its promoter (Dumont and Coker, 1986). Moreover, the immunosuppressive activity of MDSCs in EAE is inversely correlated to the degree of maturation of MDSCs (Moliné-Velázquez et al., 2014) and it is directly related to the level of Ly-6C (Zhu et al., 2007). Thus, the higher Ly-6C MFI observed in our *in vitro* studies may reflect a stronger T cell immunosuppressor activity.

Our study confirms that modifying the density of MDSCs in the spinal cord (in this case after IFN-β treatment) parallels a greater abundance of apoptotic CD4$^+$ T cells (Moliné-Velázquez et al., 2011) and that it is related to fewer CD3$^+$ T cells in the spleen. Likewise, our qualitative observations on the spinal cord tissue were corroborated *in vitro*, given the higher immunosuppressive ability of MDSCs isolated from EAE-IFN-β mice than those from EAE-Veh mice. In support of this

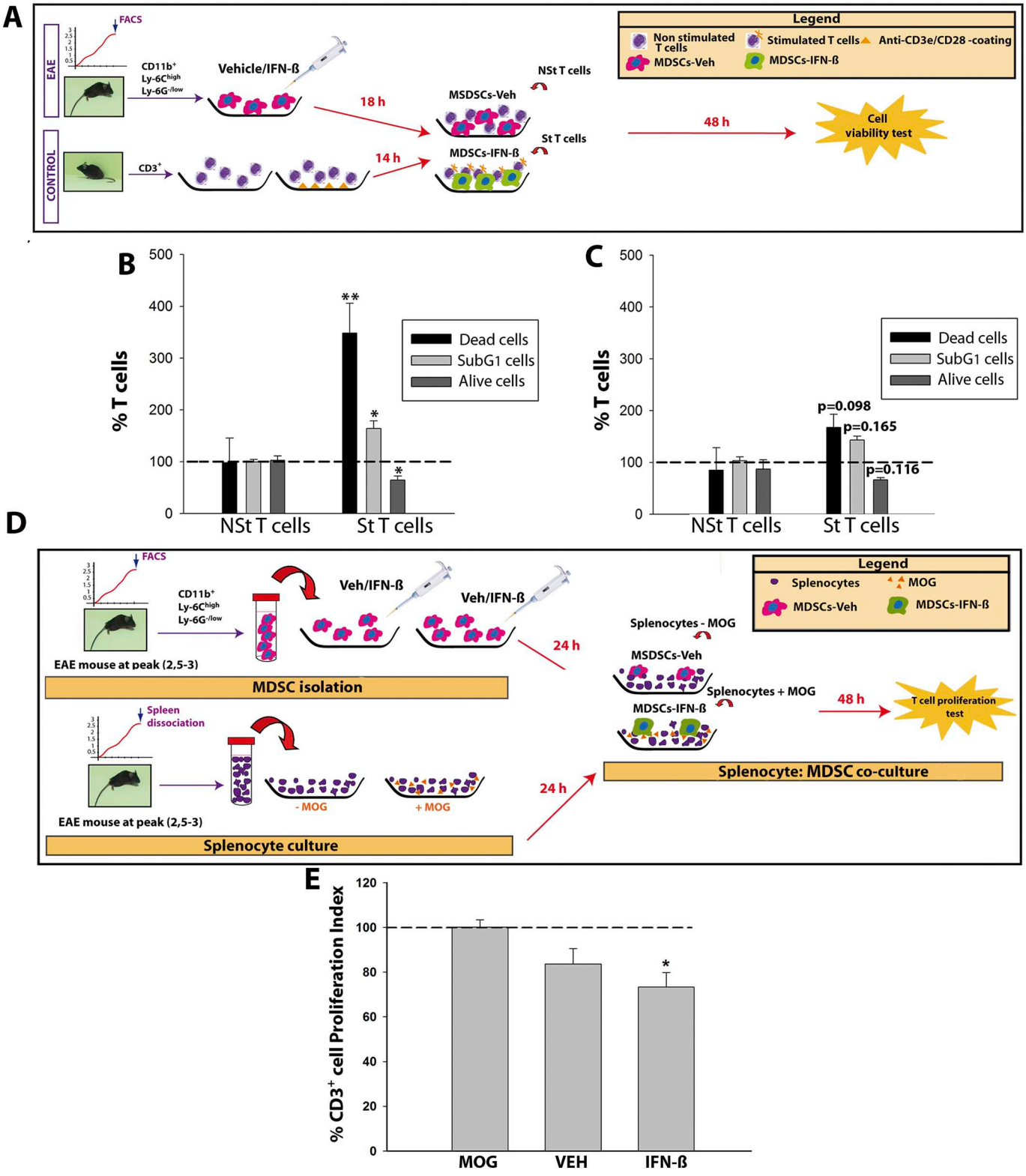

Fig. 10. MDSCs ability to suppress T cells is enhanced when pre-treated with IFN-ß, both in an unspecific and specific way. A: Layout of the co-culture protocol and IFN-ß treatment quantified in B-C. MDSCs were sorted from the spleens of EAE mice (clinical score ≥ 3.0) and treated with the vehicle alone (MDSCs-Veh) or IFN-β (MDSCs-IFN-β) for 18 h. After the culture medium was refreshed, MDSCs were exposed to control or anti-CD3e/CD28 stimulated T cells sorted from non-immunized mice in different proportions (D, 1:4; E, 1:10; MDSCs:T cells). B-C. MDSCs-IFN-ß significantly increased the dead or apoptotic (SubG1 phase) T cells compared to MDSCs-Veh when co-cultured in a 1:4 proportion (C). The same experiment was carried out at 1:10 proportion showing a trend towards a similar effect (C). D: Layout of the co-culture protocol and IFN-ß treatment. MDSCs were sorted from the spleens of EAE mice (clinical score ≥ 3.0) and treated with the vehicle alone (MDSCs-Veh) or IFN-β (MDSCs-IFN-β) for 24 h. After the culture medium was refreshed, MDSCs were exposed to control or splenic MOG stimulated T cells from EAE mice at the peak of the disease (clinical score ≥ 3.0) in a proportion of 1:4 (MDSCs:splenocytes). E: MDSCs-IFN-β, but not MDSCs-Veh, elicited a decrease in the proliferation of MOG-stimulated T cells. Abbreviations: NSt, unstimulated T cells; St, stimulated T cells. n = 5/group in A-C, n = 3/group in D-E.

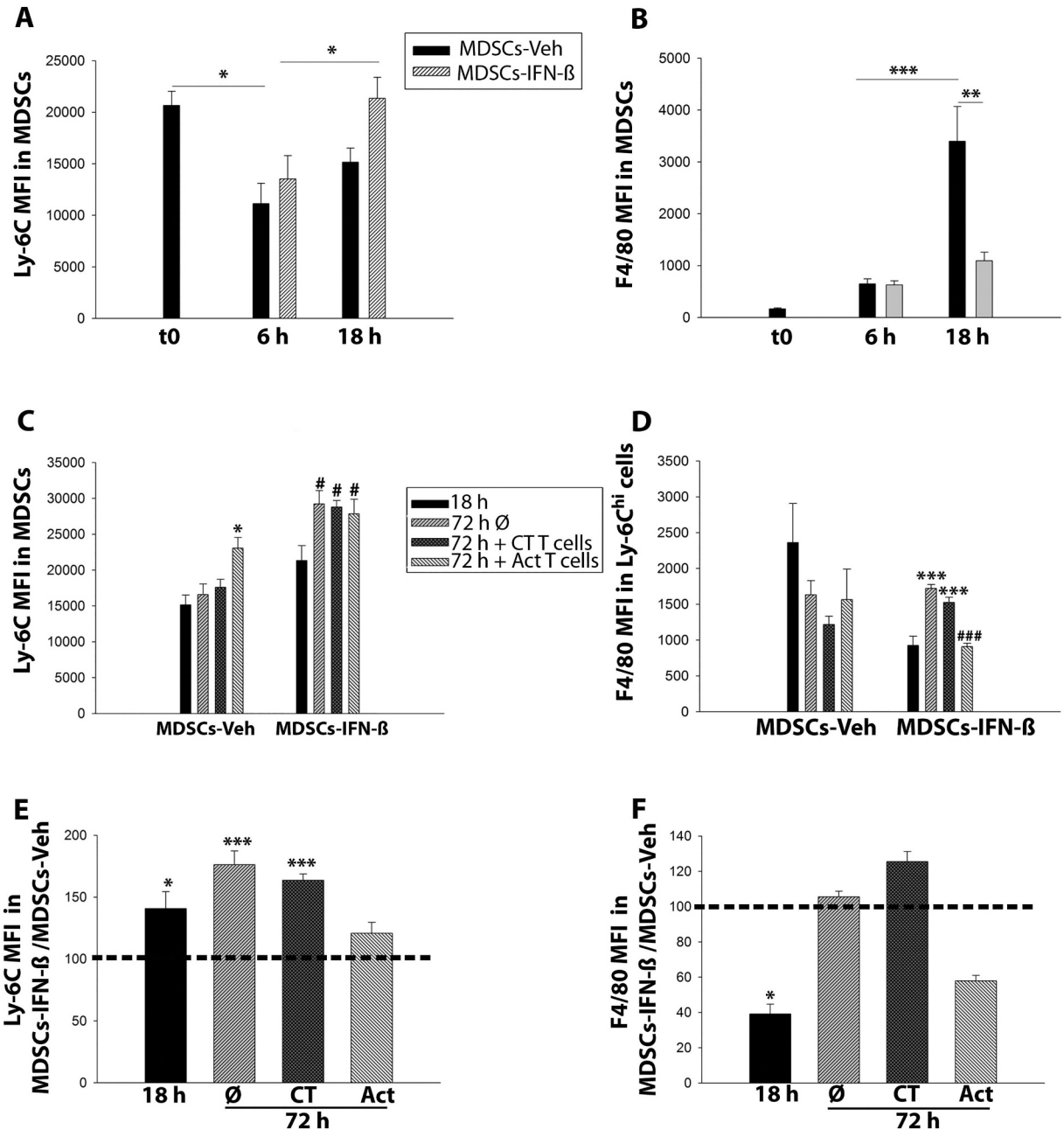

Fig. 11. IFN-ß maintains the immunosuppressor capacity of MDSCs by impairing MDSC maturation. A-B. Time course of Ly-6C (A) and F4/80 (B) MFI ratios as a respective measure of identity and immaturity of MDSCs cultured with (MDSCs-IFN-ß) or without IFN-ß (MDSCs-Veh) for 18 h. IFN-ß was effective in preserving the Ly-6C expression to levels of untreated sorted MDSCs (A). IFN-ß also prevented the differentiation of MDSCs in culture, as F4/80 expression was significantly inhibited in the IFN-β treated conditions (B). C-F. Histogram showing the MFI of Ly-6C and F4/80 in MDSCs-Veh and MDSCs-IFN-β after 48 h of co-culture with control/activated T cells, or alone. The data is presented as the absolute numbers (C and D) or for MDSCs-IFN-β relative to the MDSCs-Veh (E and F). The Ly-6C MFI from MDSCs-Veh only increased in the presence of activated T cells (*$p < .05$). By contrast, IFN-β treatment induced a stronger increase in Ly-6C MFI when the MDSCs were cultured alone or together with control/activated T cells (C; #$p < .05$). The F4/80 MFI was not significantly different between the groups after treatment with the vehicle alone. By contrast, exposure to IFN-β induced a stronger F4/80 MFI irrespective of the culture conditions (MDSCs alone or in contact with control/activated T cells) (D). Asterisks represent significant differences ($p < .001$) of the corresponding bar compared to MDSCs cultured alone during 18 h; hashes represent significant differences ($p < .001$) compared to MDSCs cultured during 72 h at all conditions. E-F: Histograms showing the MFI ratios of the Ly-6C and F4–80 markers reached by MDSCs-IFN-ß compared to MDSCS-Veh (dashed line). MDSCs-IFN-β showed a higher Ly-6C MFI at the end of the treatment, 48 h later or in the presence of control T cells, yet it was similar in the presence of activated T cells (E).The significantly lower F4/80 MFI observed in MDSCs at the end of the IFN-β-pretreatment was not detected in the rest of culture conditions (F). Abbreviations: Ø, MDSCs cultured alone; Act, MDSCs cultured with activated T cells; CT, MDSCs cultured with control T cells. MDSCs-Veh n = 5; MDSCs-IFN-ß n = 5.

model, IFN-ß dampened Gr-1 expression and it enhanced the intensity of CD124 (IL4-Rα) staining, a sign of T cell apoptosis in EAE (Moliné-Velázquez et al., 2014; Zhu et al., 2007) and cancer (Gallina et al., 2006; Mandruzzato et al., 2009). Indeed, $CD124^+$ cells have proven to be crucial in other anti-inflammatory aspects and for tissue-repair (*i.e.*: as inducers of remyelination), reinforcing the pro-regenerative role of IL4-Rα in myeloid cells (Psachoulia et al., 2016).

Our *in vitro* data suggest that IFN-β promotes the immunosuppressive activity of MDSCs independently of the inflammatory environment. As mentioned, IFN-ß suppresses the proliferation of Th1

cells (Teige et al., 2006), preventing the proliferation but not the viability of this cell type. However, we do not only demonstrate a decrease in the number of proliferative cells but also, an increase in the dead and apoptotic cells, as demonstrated when MDSCs were isolated from the spinal cord of EAE mice and co-cultured them with T cells (Moliné-Velázquez et al., 2011). On the other hand, our *in vitro* data adds new insights into the influence of the environment in which the MDSCs develop on their immunosuppressor activity, prompting us to propose the following model: the presence of T cells stimulates the anti-inflammatory properties of MDSCs and blocks their maturation towards pro-inflammatory phenotypes. Furthermore, this physiological interaction is potentiated by the IFN-β. Further research is needed to determine the exact MDSC phenotype in humans and how these cells control the immune response in MS. To date, the participation of the different MDSC subsets in MS remains controversial. On the one hand, PMN-MDSCs are the preponderant subset in RRMS patients, with little or no participation of M-MDSCs (Ioannou et al., 2012). On the other hand, M-MDSCs were shown to be the only subset that decreased in RRMS (Cantoni et al., 2017). Moreover, there was no difference in the absolute number or percentage of MDSCs or of different MDSC subsets between untreated subjects or RRMS patients treated with the disease-modifying drug, glatiramer acetate in this latter study. However, there are no reports about the number of MDSCs or the modification of the activity of these cells in MS patients treated with other compounds available in the clinic, including IFN-β. However, several studies have demonstrated the anti-inflammatory effects of IFN-β in RRMS patients, hindering T cell activation (Rudick et al., 1993), preventing pro-inflammatory immune cells from crossing the BBB, and dampening the ability of APCs to stimulate T cells (Dhib-Jalbut and Marks, 2010).

Based on our findings, we propose here that MDSCs might be considered a new endogenous cellular target for IFN-β. In the continued search for more effective therapeutic approaches for MS, MDSCs potentiated by IFN-β may be used as autologous agents to reduce the length of relapses and disease aggressiveness. In this respect, isolated MDSCs from RRMS patients may be potentiated *ex vivo* with the drug and then later autografted, thereby increasing the beneficial effects of IFN-ß and considerably limiting the side effects of this agent. Moreover, this possible *ex vivo* cell therapy might allow the clinical dose given to the patients to be reduced or even avoided, further diminishing the side effects of the drug (de Jong et al., 2017). Regarding patients that do not respond to IFN-β, here we establish the basis to by-pass this failure in the response to IFN-β through the exogenous administration of this cytokine directly on MDSCs *in vitro* before their grafting into the bloodstream.

5. Conclusions

The data presented here represent the first demonstration that the quantity and the immunosuppressive activity of MDSCs appears up-regulated after IFN-ß treatment. A single dose of IFN-ß after the first disease symptoms significantly ameliorated the clinical course of EAE, and it was associated with the enrichment in IFNAR-expressing MDSCs in both the peripheral immune system and the CNS. Besides, after IFN-β treatment, MDSCs showed a polarized stronger immunosuppressor phenotype, as shown by a reduction and an increase in the Gr-1/MHC-II and CD124/PD-L1 labeling, respectively. Furthermore, not only the phenotype but the immunosuppressive capacity of MDSCs over T cells was demonstrated to be potentiated after IFN-ß both *in vivo* and *in vitro*, an effect that was produced *via* a mechanism that may be associated with the prevention of MDSC maturation. All these data open the possibility of a future MS therapy based on autologous grafting of *ex vivo* potentiated MDSCs, reducing or even avoiding the side effects of current IFN-β therapy while selectively retaining the benefits of this compound.

Supplementary data to this article can be found online at https://doi.org/10.1016/j.nbd.2019.02.014.

Funding

This work was supported by the Spanish *Ministerio de Economía, Industria y Competitividad-MINEICO* (SAF2012-40023; SAF2016-77575-R; RD12-0032-12; RD16-0015-0019; PI15-00963; PI18/00357, partially financed by F.E.D.E.R.: European Union, "*Una Manera de hacer Europa*"), the Spanish Research Council/*Consejo Superior de Investigaciones Científicas-CSIC* (CSIC-2015201023), ADEM-TO (Spain) and ARSEP Foundation (France). DC, RL-G and IM-D were financed by SESCAM; CM-J holds a predoctoral Research Training contract from MINEICO (BES-2013-062630, –associated to SAF2012-40023 and PI15-00963) and is currently hired under SAF2016-77577-R. Dr. Clemente's group was sponsored by *Aciturri Aeronáutica SLU*, *Vesuvius Ibérica LA* and *Fundación Galletas Coral*.

Declarations of interest

None.

Acknowledgements

The authors would like to thank Dr. Virgina Vila-del Sol for her help with the flow cytometry analysis, Dr. José Ángel Rodríguez-Alfaro and Dr. Javier Mazarío for their assistance with the confocal imaging and Iris Sánchez-Raya, Aitana Alonso-Gómez and Águeda Ferrer for their technical assistance.

References

Alabanza, L.M., Esmon, N.L., Esmon, C.T., Bynoe, M.S., 2013. Inhibition of endogenous activated protein C attenuates experimental autoimmune encephalomyelitis by inducing myeloid-derived suppressor cells. J. Immunol. 191, 3764–3777.

Arnason, B.G., 2005. Long-term experience with interferon beta-1b (Betaferon)in multiple sclerosis. J. Neurol. 252 (Suppl. 3), iii28–iii33.

Brendecke, S.M., Prinz, M., 2012. How type I interferons shape myeloid cell function in CNS autoimmunity. J. Leukoc. Biol. 92, 479–488.

Bronte, V., Brandau, S., Chen, S.H., Colombo, M.P., Frey, A.B., Greten, T.F., Mandruzzato, S., Murray, P.J., Ochoa, A., Ostrand-Rosenberg, S., Rodriguez, P.C., Sica, A., Umansky, V., Vonderheide, R.H., Gabrilovich, D.I., 2016. Recommendations for myeloid-derived suppressor cell nomenclature and characterization standards. Nat. Commun. 7, 12150.

Brown, W.M., 2007. Treating COPD with PDE 4 inhibitors. Int. J. Chron. Obstruct. Pulmon. Dis. 2, 517–533.

Butovsky, O., Siddiqui, S., Gabriely, G., Lanser, A.J., Dake, B., Murugaiyan, G., Doykan, C.E., Wu, P.M., Gali, R.R., Iyer, L.K., Lawson, R., Berry, J., Krichevsky, A.M., Cudkowicz, M.E., Weiner, H.L., 2012. Modulating inflammatory monocytes with a unique microRNA gene signature ameliorates murine ALS. J. Clin. Invest. 122, 3063–3087.

Campillo, J.A., Pelaez, B., Angulo, I., Bensussan, A., Subiza, J.L., 2006. Involvement of IFNbeta on IFNgamma and nitric oxide (NO) production by bone marrow (BM) cells in response to lipopolysaccharide. Biomed. Pharmacother. 60, 541–547.

Cantoni, C., Cignarella, F., Ghezzi, L., Mikesell, B., Bollman, B., Berrien-Elliott, M.M., Ireland, A.R., Fehniger, T.A., Wu, G.F., Piccio, L., 2017. Mir-223 regulates the number and function of myeloid-derived suppressor cells in multiple sclerosis and experimental autoimmune encephalomyelitis. Acta Neuropathol. 133, 61–77.

Casacuberta-Serra, S., Costa, C., Eixarch, H., Mansilla, M.J., Lopez-Estevez, S., Martorell, L., Pares, M., Montalban, X., Espejo, C., Barquinero, J., 2016. Myeloid-derived suppressor cells expressing a self-antigen ameliorate experimental autoimmune encephalomyelitis. Exp. Neurol. 286, 50–60.

Casacuberta-Serra, S., Pares, M., Golbano, A., Coves, E., Espejo, C., Barquinero, J., 2017. Myeloid-derived suppressor cells can be efficiently generated from human hematopoietic progenitors and peripheral blood monocytes. Immunol. Cell Biol. 95, 538–548.

Cheng, W., Zhao, Q., Xi, Y., Li, C., Xu, Y., Wang, L., Niu, X., Wang, Z., Chen, G., 2015. IFN-beta inhibits T cells accumulation in the central nervous system by reducing the expression and activity of chemokines in experimental autoimmune encephalomyelitis. Mol. Immunol. 64, 152–162.

Cleveland, M.G., Lane, R.G., Klimpel, G.R., 1988. Spontaneous IFN-beta production. A common feature of natural suppressor systems. J. Immunol. 141, 2043–2049.

Comi, G., Filippi, M., Barkhof, F., Durelli, L., Edan, G., Fernandez, O., Hartung, H., Seeldrayers, P., Sorensen, P.S., Rovaris, M., Martinelli, V., Hommes, O.R., 2001. Effect of early interferon treatment on conversion to definite multiple sclerosis: a randomised study. Lancet 357, 1576–1582.

de Jong, H.J.I., Kingwell, E., Shirani, A., Cohen Tervaert, J.W., Hupperts, R., Zhao, Y., Zhu, F., Evans, C., van der Kop, M.L., Traboulsee, A., Gustafson, P., Petkau, J., Marrie, R.A., Tremlett, H., 2017. Evaluating the safety of beta-interferons in MS: a series of nested case-control studies. Neurology 88, 2310–2320.

Dhib-Jalbut, S., Marks, S., 2010. Interferon-beta mechanisms of action in multiple sclerosis. Neurology 74 (Suppl. 1), S17–S24.
Dolcetti, L., Peranzoni, E., Ugel, S., Marigo, I., Fernandez, G.A., Mesa, C., Geilich, M., Winkels, G., Traggiai, E., Casati, A., Grassi, F., Bronte, V., 2010. Hierarchy of immunosuppressive strength among myeloid-derived suppressor cell subsets is determined by GM-CSF. Eur. J. Immunol. 40, 22–35.
Dumont, F.J., Coker, L.Z., 1986. Interferon-alpha/beta enhances the expression of Ly-6 antigens on T cells in vivo and in vitro. Eur. J. Immunol. 16, 735–740.
Gabrilovich, D.I., Ostrand-Rosenberg, S., Bronte, V., 2012. Coordinated regulation of myeloid cells by tumours. Nat. Rev. Immunol. 12, 253–268.
Galligan, C.L., Pennell, L.M., Murooka, T.T., Baig, E., Majchrzak-Kita, B., Rahbar, R., Fish, E.N., 2010. Interferon-beta is a key regulator of proinflammatory events in experimental autoimmune encephalomyelitis. Mult. Scler. 16, 1458–1473.
Gallina, G., Dolcetti, L., Serafini, P., De, S.C., Marigo, I., Colombo, M.P., Basso, G., Brombacher, F., Borrello, I., Zanovello, P., Bicciato, S., Bronte, V., 2006. Tumors induce a subset of inflammatory monocytes with immunosuppressive activity on CD8+ T cells. J. Clin. Invest. 116, 2777–2790.
Giles, D.A., Washnock-Schmid, J.M., Duncker, P.C., Dahlawi, S., Ponath, G., Pitt, D., Segal, B.M., 2018. Myeloid cell plasticity in the evolution of central nervous system autoimmunity. Ann. Neurol. 83, 131–141.
Glenn, J.D., Smith, M.D., Calabresi, P.A., Whartenby, K.A., 2014. Mesenchymal stem cells differentially modulate effector CD8+ T cell subsets and exacerbate experimental autoimmune encephalomyelitis. Stem Cells 32, 2744–2755.
Gomez, A., Espejo, C., Eixarch, H., Casacuberta-Serra, S., Mansilla, M.J., Sanchez, R., Pereira, S., Lopez-Estevez, S., Gimeno, R., Montalban, X., Barquinero, J., 2014. Myeloid-derived suppressor cells are generated during retroviral transduction of murine bone marrow. Cell Transplant. 23, 73–85.
Hu, L., Huang, W., Hjort, E.E., Bei, L., Platanias, L.C., Eklund, E.A., 2016. The interferon consensus sequence binding protein (Icsbp/Irf8) is required for termination of emergency granulopoiesis. J. Biol. Chem. 291, 4107–4120.
Iacobaeus, E., Douagi, I., Jitschin, R., Marcusson-Stahl, M., Andren, A.T., Gavin, C., Lefsihane, K., Davies, L.C., Mougiakakos, D., Kadri, N., Le, B.K., 2018. Phenotypic and functional alterations of myeloid-derived suppressor cells during the disease course of multiple sclerosis. Immunol. Cell Biol. 96, 820–830.
Ioannou, M., Alissafi, T., Lazaridis, I., Deraos, G., Matsoukas, J., Gravanis, A., Mastorodemos, V., Plaitakis, A., Sharpe, A., Boumpas, D., Verginis, P., 2012. Crucial role of granulocytic myeloid-derived suppressor cells in the regulation of central nervous system autoimmune disease. J. Immunol. 188, 1136–1146.
Jankovic, S.M., 2010. Injectable interferon beta-1b for the treatment of relapsing forms of multiple sclerosis. J. Inflamm. Res. 3, 25–31.
Kasper, L.H., Reder, A.T., 2014. Immunomodulatory activity of interferon-beta. Ann. Clin. Transl. Neurol. 1, 622–631.
Kavrochorianou, N., Evangelidou, M., Markogiannaki, M., Tovey, M., Thyphronitis, G., Haralambous, S., 2016. IFNAR signaling directly modulates T lymphocyte activity, resulting in milder experimental autoimmune encephalomyelitis development. J. Leukoc. Biol. 99, 175–188.
Kieseier, B.C., 2011. The mechanism of action of interferon-beta in relapsing multiple sclerosis. CNS Drugs 25, 491–502.
King, I.L., Dickendesher, T.L., Segal, B.M., 2009. Circulating Ly-6C+ myeloid precursors migrate to the CNS and play a pathogenic role during autoimmune demyelinating disease. Blood 113, 3190–3197.
Kohanbash, G., McKaveney, K., Sakaki, M., Ueda, R., Mintz, A.H., Amankulor, N., Fujita, M., Ohlfest, J.R., Okada, H., 2013. GM-CSF promotes the immunosuppressive activity of glioma-infiltrating myeloid cells through interleukin-4 receptor-alpha. Cancer Res. 73, 6413–6423.
Koutrolos, M., Berer, K., Kawakami, N., Wekerle, H., Krishnamoorthy, G., 2014. Treg cells mediate recovery from EAE by controlling effector T cell proliferation and motility in the CNS. Acta Neuropathol. Commun. 2, 163.
Kozovska, M.E., Hong, J., Zang, Y.C., Li, S., Rivera, V.M., Killian, J.M., Zhang, J.Z., 1999. Interferon beta induces T-helper 2 immune deviation in MS. Neurology 53, 1692–1697.
Mandruzzato, S., Solito, S., Falisi, E., Francescato, S., Chiarion-Sileni, V., Mocellin, S., Zanon, A., Rossi, C.R., Nitti, D., Bronte, V., Zanovello, P., 2009. IL4Ralpha+ myeloid-derived suppressor cell expansion in cancer patients. J. Immunol. 182, 6562–6568.
Martin-Saavedra, F.M., Flores, N., Dorado, B., Eguiluz, C., Bravo, B., Garcia-Merino, A., Ballester, S., 2007. Beta-interferon unbalances the peripheral T cell proinflammatory response in experimental autoimmune encephalomyelitis. Mol. Immunol. 44, 3597–3607.
Mastorodemos, V., Ioannou, M., Verginis, P., 2015. Cell-based modulation of autoimmune responses in multiple sclerosis and experimental autoimmmune encephalomyelitis: therapeutic implications. Neuroimmunomodulation 22, 181–195.
Mastronardi, F.G., Min, W., Wang, H., Winer, S., Dosch, M., Boggs, J.M., Moscarello, M.A., 2004. Attenuation of experimental autoimmune encephalomyelitis and non-immune demyelination by IFN-beta plus vitamin B12: treatment to modify notch-1/sonic hedgehog balance. J. Immunol. 172, 6418–6426.
Melero-Jerez, C., Ortega, M.C., Moliné-Velázquez, V., Clemente, D., 2016. Myeloid derived suppressor cells in inflammatory conditions of the central nervous system. Biochim. Biophys. Acta 1862, 368–380.
Meyer, C., Martin-Blondel, G., Liblau, R.S., 2017. Endothelial cells and lymphatics at the interface between the immune and central nervous systems: implications for multiple sclerosis. Curr. Opin. Neurol. 30, 222–230.
Mildner, A., Mack, M., Schmidt, H., Bruck, W., Djukic, M., Zabel, M.D., Hille, A., Priller, J., Prinz, M., 2009. CCR2+Ly-6Chi monocytes are crucial for the effector phase of autoimmunity in the central nervous system. Brain 132, 2487–2500.
Moliné-Velázquez, V., Cuervo, H., Vila del Sol, V., Ortega, M.C., Clemente, D., de Castro, F., 2011. Myeloid-derived suppressor cells limit the inflammation by promoting T lymphocyte apoptosis in the spinal cord of a murine model of multiple sclerosis. Brain Pathol. 21, 678–691.
Moliné-Velázquez, V., Ortega, M.C., Vila del Sol, V., Melero-Jerez, C., de Castro, F., Clemente, D., 2014. The synthetic retinoid Am80 delays recovery in a model of multiple sclerosis by modulating myeloid-derived suppressor cell fate and viability. Neurobiol. Dis. 67, 149–164.
Moliné-Velázquez, V., Vila-del, Sol, de Castro, F., Clemente, D., 2016. Myeloid cell distribution and activity in multiple sclerosis. Histol. Histopathol. 31, 357–370.
Movahedi, K., Guilliams, M., Van den, B.J., Van den, B.R., Gysemans, C., Beschin, A., De, B.P., Van Ginderachter, J.A., 2008. Identification of discrete tumor-induced myeloid-derived suppressor cell subpopulations with distinct T cell-suppressive activity. Blood 111, 4233–4244.
Ortega, S.B., Kashi, V.P., Tyler, A.F., Cunnusamy, K., Mendoza, J.P., Karandikar, N.J., 2013. The disease-ameliorating function of autoregulatory CD8 T cells is mediated by targeting of encephalitogenic CD4 T cells in experimental autoimmune encephalomyelitis. J. Immunol. 191, 117–126.
Parekh, V.V., Wu, L., Olivares-Villagómez, D., Wilson, K.T., Van, K.L., 2013. Activated invariant NKT cells control central nervous system autoimmunity in a mechanism that involves myeloid-derived suppressor cells. J. Immunol. 190, 1948–1960.
Pogue, S.L., Preston, B.T., Stalder, J., Bebbington, C.R., Cardarelli, P.M., 2004. The receptor for type I IFNs is highly expressed on peripheral blood B cells and monocytes and mediates a distinct profile of differentiation and activation of these cells. J. Interf. Cytokine Res. 24, 131–139.
Prinz, M., Schmidt, H., Mildner, A., Knobeloch, K.P., Hanisch, U.K., Raasch, J., Merkler, D., Detje, C., Gutcher, I., Mages, J., Lang, R., Martin, R., Gold, R., Becher, B., Bruck, W., Kalinke, U., 2008. Distinct and nonredundant in vivo functions of IFNAR on myeloid cells limit autoimmunity in the central nervous system. Immunity 28, 675–686.
Psachoulia, K., Chamberlain, K.A., Heo, D., Davis, S.E., Paskus, J.D., Nanescu, S.E., Dupree, J.L., Wynn, T.A., Huang, J.K., 2016. IL4I1 augments CNS remyelination and axonal protection by modulating T cell driven inflammation. Brain 139, 3121–3136.
Rudick, R.A., Carpenter, C.S., Cookfair, D.L., Tuohy, V.K., Ransohoff, R.M., 1993. In vitro and in vivo inhibition of mitogen-driven T-cell activation by recombinant interferon beta. Neurology 43, 2080–2087.
Saederup, N., Cardona, A.E., Croft, K., Mizutani, M., Cotleur, A.C., Tsou, C.L., Ransohoff, R.M., Charo, I.F., 2010. Selective chemokine receptor usage by central nervous system myeloid cells in CCR2-red fluorescent protein knock-in mice. PLoS.One. 5, e13693.
Salama, A.D., Chitnis, T., Imitola, J., Ansari, M.J., Akiba, H., Tushima, F., Azuma, M., Yagita, H., Sayegh, M.H., Khoury, S.J., 2003. Critical role of the programmed death-1 (PD-1) pathway in regulation of experimental autoimmune encephalomyelitis. J. Exp. Med. 198, 71–78.
Scheller, M., Foerster, J., Heyworth, C.M., Waring, J.F., Lohler, J., Gilmore, G.L., Shadduck, R.K., Dexter, T.M., Horak, I., 1999. Altered development and cytokine responses of myeloid progenitors in the absence of transcription factor, interferon consensus sequence binding protein. Blood 94, 3764–3771.
Schreiber, G., 2017. The molecular basis for differential type I interferon signaling. J. Biol. Chem. 292, 7285–7294.
Serbina, N.V., Pamer, E.G., 2006. Monocyte emigration from bone marrow during bacterial infection requires signals mediated by chemokine receptor CCR2. Nat. Immunol. 7, 311–317.
Sonda, N., Chioda, M., Zilio, S., Simonato, F., Bronte, V., 2011. Transcription factors in myeloid-derived suppressor cell recruitment and function. Curr. Opin. Immunol. 23, 279–285.
Sospedra, M., Martin, R., 2005. Antigen-specific therapies in multiple sclerosis. Int. Rev. Immunol. 24, 393–413.
Stewart, T.J., Greeneltch, K.M., Reid, J.E., Liewehr, D.J., Steinberg, S.M., Liu, K., Abrams, S.I., 2009. Interferon regulatory factor-8 modulates the development of tumour-induced CD11b+Gr-1+ myeloid cells. J. Cell. Mol. Med. 13, 3939–3950.
Stone, L.A., Frank, J.A., Albert, P.S., Bash, C., Smith, M.E., Maloni, H., McFarland, H.F., 1995. The effect of interferon-beta on blood-brain barrier disruptions demonstrated by contrast-enhanced magnetic resonance imaging in relapsing-remitting multiple sclerosis. Ann. Neurol. 37, 611–619.
Suardíaz, M., Clemente, D., Marín-Banasco, C., Orpez, T., Hurtado-Guerrero, I., Pavia, J., Pinto-Medel, M.J., de Castro, F., Leyva, L., Fernández, O., Oliver, B., 2016. Recombinant soluble IFN receptor (sIFNAR2) exhibits intrinsic therapeutic efficacy in a murine model of multiple sclerosis. Neuropharmacology 110, 480–492.
Sunderkotter, C., Nikolic, T., Dillon, M.J., Van, R.N., Stehling, M., Drevets, D.A., Leenen, P.J., 2004. Subpopulations of mouse blood monocytes differ in maturation stage and inflammatory response. J. Immunol. 172, 4410–4417.
Sweeney, C.M., Lonergan, R., Basdeo, S.A., Kinsella, K., Dungan, L.S., Higgins, S.C., Kelly, P.J., Costelloe, L., Tubridy, N., Mills, K.H., Fletcher, J.M., 2011. IL-27 mediates the response to IFN-beta therapy in multiple sclerosis patients by inhibiting Th17 cells. Brain Behav. Immun. 25, 1170–1181.
Taleb, K., Auffray, C., Villefroy, P., Pereira, A., Hosmalin, A., Gaudry, M., Le, B.A., 2017. Chronic type I IFN is sufficient to promote immunosuppression through accumulation of myeloid-derived suppressor cells. J. Immunol. 198, 1156–1163.
Tarassishin, L., Suh, H.S., Lee, S.C., 2011. Interferon regulatory factor 3 plays an anti-inflammatory role in microglia by activating the PI3K/Akt pathway. J. Neuroinflammation 8, 187.
Teige, I., Liu, Y., Issazadeh-Navikas, S., 2006. IFN-beta inhibits T cell activation capacity of central nervous system APCs. J.Immunol. 177, 3542–3553.
Trinschek, B., Luessi, F., Gross, C.C., Wiendl, H., Jonuleit, H., 2015. Interferon-Beta therapy of multiple sclerosis patients improves the responsiveness of T cells for immune suppression by regulatory T cells. Int. J. Mol. Sci. 16, 16330–16346.
Waubant, E., Vukusic, S., Gignoux, L., Dubief, F.D., Achiti, I., Blanc, S., Renoux, C.,

Confavreux, C., 2003. Clinical characteristics of responders to interferon therapy for relapsing MS. Neurology 61, 184–189.
Weissert, R., 2017. Adaptive immunity is the key to the understanding of autoimmune and paraneoplastic inflammatory central nervous system disorders. Front. Immunol. 8, 336.
Wlodarczyk, A., Cedile, O., Jensen, K.N., Jasson, A., Mony, J.T., Khorooshi, R., Owens, T., 2015. Pathologic and protective roles for microglial subsets and bone marrow- and blood-derived myeloid cells in central nervous system inflammation. Front. Immunol. 6, 463.
Yang, R., Cai, Z., Zhang, Y., Yutzy, W.H., Roby, K.F., Roden, R.B., 2006. CD80 in immune suppression by mouse ovarian carcinoma-associated Gr-1 + CD11b + myeloid cells. Cancer Res. 66, 6807–6815.
Yi, H., Guo, C., Yu, X., Zuo, D., Wang, X.Y., 2012. Mouse CD11b + Gr-1 + myeloid cells can promote Th17 cell differentiation and experimental autoimmune encephalomyelitis. J. Immunol. 189, 4295–4304.
Youn, J.I., Nagaraj, S., Collazo, M., Gabrilovich, D.I., 2008. Subsets of myeloid-derived suppressor cells in tumor-bearing mice. J. Immunol. 181, 5791–5802.
Zhu, B., Guleria, I., Khosroshahi, A., Chitnis, T., Imitola, J., Azuma, M., Yagita, H., Sayegh, M.H., Khoury, S.J., 2006. Differential role of programmed death-ligand 1 [corrected] and programmed death-ligand 2 [corrected] in regulating the susceptibility and chronic progression of experimental autoimmune encephalomyelitis. J. Immunol. 176, 3480–3489.
Zhu, B., Bando, Y., Xiao, S., Yang, K., Anderson, A.C., Kuchroo, V.K., Khoury, S.J., 2007. CD11b + Ly-6C(hi) suppressive monocytes in experimental autoimmune encephalomyelitis. J. Immunol. 179, 5228–5237.
Zhu, B., Kennedy, J.K., Wang, Y., Sandoval-Garcia, C., Cao, L., Xiao, S., Wu, C., Elyaman, W., Khoury, S.J., 2011. Plasticity of Ly-6C(hi) myeloid cells in T cell regulation. J. Immunol. 187, 2418–2432.